Russian Chemical Reviews **80** (8) 705 – 725 (2011) © 2011 Russian Academy of Sciences and Turpion Ltd

DOI 10.1070/RC2011v080n08ABEH004232

Covalent functionalization of carbon nanotubes: synthesis, properties and applications of fluorinated derivatives †

V N Khabashesku

Contents

I.	Introduction	705
II.	Fluorination of carbon nanotubes	706
III.	Structure of fluoronanotubes	710
IV.	Solvation properties of fluoronanotubes	711
V.	Chemical properties of fluoronanotubes	712
VI.	Conclusions	722

Abstract. Chemical methods for preparation of fluorinated carbon nanotubes and their functional derivatives published over the last 10 – 15 years are considered in detail and critically analyzed. Fluorinated carbon nanotube derivatives represent a new family of nanoscale fluorocarbon materials promising new applications in nanocomposites, sensors, nanoelectronic devices, nanoengineered drug delivery systems and lubricants. The bibliography includes 166 references.

I. Introduction

Carbon nanotubes (CNTs) have been discovered in 1991 by Iijima.[1] They represent a nanocrystalline carbon clusters structurally built from graphene sheets rolled into a tube that is closed at the ends by the fullerene caps. Depending on synthesis conditions, nanotubes can be produced in a single, double or multi-walled arrangement. Single-walled nanotubes (SWCNTs) consist of a single graphene cylinder. Double- and multi-walled nanotubes (DWCNTs and MWCNTs) are consequently made of two or more concentric graphitic layers surrounding the central tubule.[2–4] Diameters of SWCNTs and DWCNTs can range from 0.4 to 4 nm and those of MWCNTs are from 4 to 100 nm. Different synthesis and purification methods yield nanotubes that can be from 100 nm to tens or even hundreds of microns long. The unique mechanical, optical, thermal and electric properties and other phenomena exhibited by carbon nanotubes offer many opportunities for their applications.[5–11] Single- and double-walled carbon nanotubes, in particular, possess a remarkable tensile strength. For this reason the potential uses of SWCNTs, DWCNTs and MWCNTs for fabrication of reinforced fibers and nanocomposites are being investigated extensively.[10–17]

CNTs tend to self-assemble into bundles in which from several tubes up to a hundred are held together by van der Waals forces. For many engineering and bio-medical applications, *e.g.*, in nanocomposites and drug delivery systems, the separation of individual nanotubes from their bundles is becoming essential. This would improve the dispersion and solubilization of the nanotubes in common organic solvents and water needed for their processing and manipulation. To solve this problem, the approaches based on non-covalent[18–25] and covalent[26–51] functionalization of nanotubes are being pursued. The covalent functionalization leads to attachment of various functional groups to the ends or sidewalls of the nanotubes through covalent bonds. Functionalization of the nanotube ends brings only a highly localized transformation of the nanotube electronic structure and does not change the bulk properties of these materials. By comparison, functionalization of the nanotube sidewalls naturally results in a significant modification of the intrinsic properties of the nanotubes.

The challenges faced in the sidewall chemical functionalization are related to a very low reactivity of the nanotubes due to a much lower curvature of nanotube graphene walls than in the fullerenes,[5] and to the necessity of preserving the tubular structure when attaching the functional groups. The carbon nanotube graphene structure, built from carbon atoms in their sp^2-bonding states, facilitates the predominant occurrence of addition reactions. For this type of reactions, gaseous fluorine serves as a reagent of choice since it easily generates highly reactive F atoms under mild conditions (F – F bond dissociation energy is only 38 kcal mol^{-1}) and therefore fluorination works as a powerful tool for covalent surface modification of carbon materials.[52]

V N Khabashesku Department of Chemical and Biomolecular Engineering, University of Houston, 4800 Calhoun blvd., 77204 Houston, TX, USA. Fax (1-713) 743 43 23, tel. (1-713) 743 89 55, e-mail: valery@uh.edu

Received 8 June 2010
Uspekhi Khimii **80** (8) 739 – 760 (2011)

† Dedicated to Academician O M Nefedov on occasion of his 80th birthday.

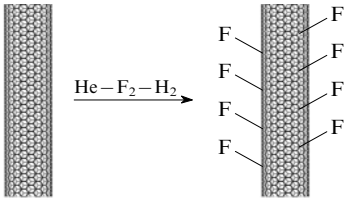
During the last decade, dozens of review articles on CNTs and their covalent functionalization have been published. Although some of these reviews briefly discuss fluoronanotubes, a detailed review entirely focused on the progress in fluorination and subsequent derivatization of CNTs did not appear in a peer-reviewed journal since 2002.[29] Fluorinated carbon nanotubes represent a new family of nanoscale fluorocarbon materials. They enable various applications of functionalized carbon nanotubes, derived from fluoronanotubes, and therefore they deserve a special place in chemistry of carbon nanotubes.

This review provides an up to date literature survey of methods and results of fluorination of single-, double- and multi-walled carbon nanotubes. This is followed by discussions of microstructure and solvation properties of fluoronanotubes formed as the result of fluorination of CNTs. The subsequent development of chemistry of fluoronanotubes as versatile precursors for synthesis of an array of functionalized nanotube derivatives is discussed in greater details. This is accompanied by outlines of documented examples showing the perspectives for applications of fluorinated CNT derivatives in nanocomposites, sensors, solid lubricants and lithium batteries.

II. Fluorination of carbon nanotubes

1. Single-walled carbon nanotubes

The direct fluorination of the SWCNTs with elementary fluorine was carried out as far back as 1998 by Margrave and coworkers[53] and became the first example of non-destructive sidewall functionalization of single-wall type of nanotubes.



They have been prepared from the SWNCTs grown by three different methods, laser ablation of graphite (L-SWNCTs),[54,55] high-pressure CO disproportionation process (HiPco-SWCNTs),[56,57] and conventional catalytic arc discharge method (Arc-SWCNTs).[58] Each of these methods yields SWCNTs of different average diameter and degree of sidewall perfection, which therefore require different conditions for direct fluorination.

By using the methodology developed earlier for the fluorination of graphite,[59] extensive fluorination studies[53,60,61] were carried out to establish optimal conditions (reaction temperatures, reaction times, addition of HF or H_2 for *in situ* generation of HF catalyst) to reach a saturation stoichiometry (nearly C_2F) without destruction of the tube structure. It was found that the degree of fluorination depends on the residual metal content from catalysts used in the purified SWCNTs and the conditions of preparation and treatment of the buckypaper samples (nature of solvent, annealing temperature) prior to fluorination.

The fluorination of L-SWCNT buckypaper, pre-baked at 1100 °C in vacuum, was carried out at temperatures ranging from 150 to 600 °C. The IR spectroscopy (KBr pellet method) confirmed the presence of covalently bound fluorine (peaks of the C−F stretches in the 1220–1250 cm^{-1} region) in the samples fluorinated in absence of HF catalyst at temperatures of 250 °C and higher, and not for those fluorinated at 150 °C. The TEM images indicated that the tube structures remain largely intact under treatment at temperatures as high as 325 °C, yielding approximately C_2F product bulk composition according to electron probe microanalysis (EPMA). This type SWCNTs are essentially all destroyed (*i.e.*, 'unzipped') when fluorinated at 400 °C and above to form a fluorographite as a main product. This does not contradict the results of semi-empirical MNDO computational modelling of fluorination of narrower (6,0), (8.0), (6,6), (7,7) and (8,8) SWCNTs predicting that nanotubes with the diameters smaller than 1 nm can form stable fluoronanotubes having fluorine atoms bonded from outside and inside to the wall at theoretically saturated C/F = 1 ratio while larger diameter SWCNTs cannot be fluorinated to that high surface saturation.[62] As a result of the sidewall functionalization of the SWCNTs by fluorine the electrical properties of the fluoronanotubes differ dramatically from those of pristine SWCNTs. The fluoronanotubes prepared by fluorination at temperatures of 250 °C and above become insulators while the pristine nanotubes are known to be good conductors.[5,6,53]

In the presence of HF, which is a known catalyst for fluorination of graphite, the saturated C/F ratio (~2) for the L-SWCNT tube structure was reached at a lower reaction temperature (250 °C) while maintaining the same reaction time (~ 5 h). The other observed effect of HF was a noticeable upshift of the C−F stretching frequency in the FTIR spectra of fluoronanotubes, which indicated the formation of more covalent and therefore stronger C−F bonds. The same upshifting effect and a higher relative intensity of the C−F band in the IR spectra were also seen when raising the fluorination temperature. These phenomena are in agreement with those observed earlier in fluorinated graphite.[59] Typically, use of lower temperatures and concentrations of F_2 for fluorination of carbon materials produces fluorocarbons in which the fluorine forms a semi-ionic bond to carbon and shows a lower ν(C−F) feature in the IR spectra than with the covalently bonded fluorine. For example, in the IR spectra of L-SWCNTs the peak due to ν(C−F) stretch shifts from 1201 to 1176 cm^{-1} when the fluorination temperature is reduced from 250 to 200 °C.[61]

The following studies,[63,64] where the vacuum annealed L-SWCNTs were fluorinated at 200–260 °C with a mixture of F_2 (20%) and N_2 (80%), have demonstrated the efficient use of combination of X-ray photoelectron spectroscopy (XPS), Raman and IR spectroscopy[63] for determination of the fluorination stoichiometry C_nF and nature of the fluorine bonding in fluoronanotubes.[64] In the XPS C1s spectra of fluronanotubes of $CF_{0.43}$ (close to about C_2F) stoichiometry two main peaks were detected at 286.0 and 288.7 ± 0.3 eV, which were attributed to a carbon bonded to monofluorinated carbon (C−CF_1) and carbon bonded to a single F atom (CF_1) predominantly by a covalent bond, respectively. The integrated intensities of these peaks were 53 : 47, in accord with the observed stoichiometry. The F1s binding energy in XPS of this fluoronanotubes sample was 687.8 ± 0.3 eV (Ref. 64) which is typically observed for fluorine covalently bonded to carbon.[52] On the other hand, for fluoronanotubes, prepared from the L-SWCNT

buckypaper vacuum-baked at temperature as high as 1250 °C, the F1s peak was observed at a lower binding energy (683.8 eV) suggesting a more ionic character of the C–F bond in this sample.[63]

Fluorination was performed for open- and closed-end L-SWCNTs (o-SWCNTs and c-SWCNTs) by direct reaction with elemental 1 atm F_2 gas at 300, 473 and 523 K for 1 month, 5 h and 5 h, respectively.[65] The XPS analysis has shown the highest fluorine content in the samples fluorinated at 523 K ($F/C \approx 0.5$), in agreement with the previous results of fluorination of L-SWCNTs with a continuous flow of F_2 gas diluted by helium to a low partial pressure ($\sim$0.09 atm).[61] Structural changes of SWCNTs by fluorination were studied by XRD and Raman measurements. Interestingly, the lattice constants calculated from XRD patterns for the fluorinated c-SWCNTs were larger than the lattice constants for o-SWCNTs at the same fluorine content. Also, complete disappearance of radial breathing mode (RBM) peaks in the Raman spectrum of c-SWCNTs with $F/C = 0.48$ has been observed while in the case of o-SWCNT RBMs were observed even for the sample with the highest fluorine content ($F/C = 0.51$). These data were interpreted by the selective fluorination occurring entirely on the outside of c-SWCNT tubes and resulting in a larger lattice constant than fluorinated o-SWCNT with the same F/C value where some fluorine atoms are attached to the inner and outer sides of the same areas of the wall, leaving a larger area of the wall less affected by fluorination.[65]

The HiPco-SWCNTs have a smaller average diameters [$\sim$1 nm for the (8,8) nanotubes] than L-SWCNTs [$\sim$1.4 nm, corresponding to the (10,10) tubes] and, therefore, due to a higher curvature, they are more reactive. This is particularly indicated by the observation that under the same fluorination conditions more fluorine can be attached onto the sidewalls of HiPco-SWCNTs.[61] For instance, in the presence of HF the near C_2F composition for the tubular structure of the HiPco-SWCNTs has been produced at a fluorination temperature as low as 150 °C, while under the same conditions the L-SWCNTs yielded the fluoronanotubes with significantly lower fluorine content (C/F ratio higher than 3). The fluoronanotubes with a stoichiometry of C_5F were produced by controlling the conditions of fluorination through adjusting the flow rates of F_2 and helium so that in the gas mixture the concentration of F_2 was about 1%. The controlled temperature and reaction time have been maintained at 50 ± 5 °C and 2 h, respectively.[29, 66]

HiPco-SWCNTs have also been fluorinated at room temperature using a volatile mixture of BrF_3 and Br_2.[67] According to XPS analysis, the composition of the fluoronanotubes obtained was C_4F. Raman spectroscopy showed that the narrower tubes are more readily fluorinated. Comparison between CK_α-spectrum of the fluorinated SWCNTs and theoretical spectra obtained for the (8,8) tube models with different fluorine adiition patterns revealed the fluorine atoms preferably forming the chains around a tube circumference. The same fluorination technique was applied to a pristine and ball-milled samples containing SWCNTs and few-wall carbon nanotubes (FWCNTs) produced by catalytic CVD method.[68] Analysis of the XPS C1s spectra revealed that fluorinated carbon atoms in SWCNTs are bounded with at least one C–F group while most of the fluorinated carbon atoms in FWCNTs are surrounded by bare carbon atoms only. It was found that ball-milling of the samples has insignificant effect on CNT length and most likely produces defects in CNT surface layers. These defects provide access for fluorine atoms to the subsurface layers of FWCNTs which results in increase of fluorine content in the milled sample. Near-edge X-ray absorption fine structure (NEXAFS) spectroscopic investigation revealed that some of CNTs, which probably constitute the interior of FWCNTs or CNT ropes, are not fluorinated under the conditions used and the fluorine atoms interact more strongly with CNT surfaces having a larger curvature.

High-resolution TEM images (Fig. 1) show significantly different surface morphology for fluoronanotubes sample in comparison with the pristine SWCNTs. Smooth sidewall surfaces of thick SWCNT bundles (see Fig. 1 *a*) change to a 'bumpy' appearance after the fluorination (see Fig. 1 *b*); this can be related to a great number of sp^3 carbon–carbon bonds formed *via* addition of fluorine. Significant reduction in bundle size is also noted for the fluoronanotubes (see Fig. 1 *b*) where this effect is usually proportional to the degree of fluorination; for example, 2–3 times larger size bundles are observed for $C_{20}F$ than for C_5F and C_2F F-SWCNTs.[69] This difference has likely been the reason for very low friction coefficient (0.002) measured during tribology tests for $C_{20}F$ nanotubes as compared to higher fluorinated SWCNTs. This can be due to a possibility of better intertube sliding within the bundles and less contact with the surface asperities by $C_{20}F$ solid lubricant whereas individual SWCNTs having diameters larger than surface roughness will necessarily slide between adjacent tribological surfaces. These findings are important for design and potential applications of fluorinated CNTs as very low friction solid lubricants.

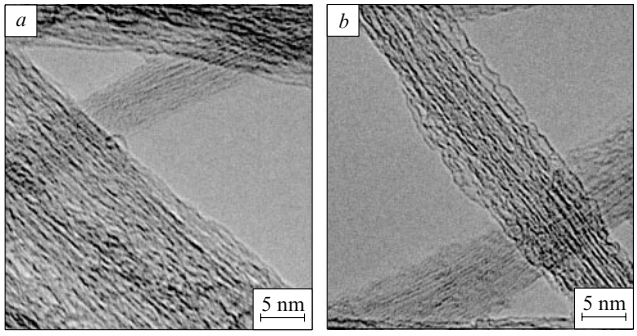


Figure 1. High resolution TEM images of SWCNT samples: (*a*) pristine SWCNTs, (*b*) fluoronanotubes.[69]

Analysis of fluorinated HiPco carbon nanotubes by magic angle spinning (MAS) NMR spectroscopy has been reported.[70] In the MAS spectra of HiPco fluoronanotubes ($C_{2.1}F$), the ^{13}C NMR shift for the sp^3 carbon bonded to fluorine was observed at 83.5 ppm, 7–15 ppm upfield of the shift typical for tertiary alkyl fluorides, while the shift for the sp^2 bonded carbon was detected at 128 ppm, customary for the nanotube sidewall. The shift observed for the sp^3 carbons in the fluoronanotubes was interpreted to be due to the C–F moieties located predominantly in 1,2- rather than 1,4-addition patterns of fluorine as confirmed by *ab initio* calculations. Based on comparison with the XPS and Raman data, the solid-state ^{13}C NMR spectroscopy has been suggested as a better tool for quantitative assessment

of the extent of fluorination of carbon nanotubes, especially for highly fluorinated samples.

The systematic studies of Arc-SWCNTs[71,72] by XPS and resistivity measurements of fluorinated powder material as a function of fluorination temperature have revealed a notable binding energy shift towards higher energies with increasing fluorination temperature. The CF_n fluoronanotubes produced at low temperatures of up to 200 °C showed an ionic character of the C–F bonds, while at higher temperatures the C–F bonds became more covalent in nature. The observed enhancement in the sp^3 bonding along with the resistivity increase was confirmed by the four-point resistivity measurements. The fluorination at temperatures above 250 °C has lead to cleavage of carbon–carbon bonds and collapse of tube structure as observed by TEM.[69,72] The XPS and Auger spectroscopy studies of Arc-SWCNTs fluorinated with 1 atm fluorine gas at room temperature for 48 hours have shown that fluorine forms only one chemical state for the C–F bonding in the fluoronanotubes obtained.[73]

The fluorination of Arc-SWCNTs with 1.5 nm average diameter was carried out at temperatures ranging from 150 to 300 °C with undiluted fluorine gas filled into a stainless steel reactor up to a pressure of 0.8 bar.[74] The maximum weight uptake by this type of SWCNTs corresponding to $\sim CF_{0.44}$ stoichiometry, which is close to the theoretically attainable limit of $CF_{0.5}$, was obtained at temperature of $\sim$ 190 °C and 5 h fluorination time. It was shown by TEM studies that in comparison with L-SWCNTs, fluorinated under a low fluorine pressure of 0.09 bar and temperature of 250 °C,[60] fluorination of Arc-SWCNTs at 220 °C can already lead to partial decomposition of nanotube bundles which emphasizes the need for use of lower temperatures under increased fluorine pressure to retain SWCNT structure. Characterization of fluoronanotubes by MAS (^{13}C, ^{19}F) NMR, IR, X-ray absorption and photoelectron spectroscopies have provided convincing evidences for C–F covalent bonding.

Fluorination studies of SWCNTs using fluorine gas molecules have experimentally proven that metallic nanotubes are more reactive than the semiconducting ones towards strong electron acceptors capable of large charge transfer, such as halogens.[75] It was particularly found that at room temperature SWCNTs with radii between 0.9 and 1.1 nm are predominantly etched. Such difference in reactivity is guided by the electron density of states at the Fermi level being responsible for energy bandgap of the nanotubes. The observed selective etching of metallic tubes by reacting SWCNTs with fluorine was proposed as a tool for separation of semiconducting nanotubes. The obtained results were consistent with the *ab initio* calculations[76] suggesting that low-temperature exposure to F_2 molecules in the gas phase should result in high yield of fluorinated metallic SWCNTs while semiconducting nanotubes will remain unfluorinated. These calculations also predict that under low temperature conditions the metallic nanotubes with radii larger than $\sim$1.3 nm will be mostly etched.

Besides reactions with F_2 discussed above, the fluorination process of SWCNTs by reactive species generated from CF_4 in microwave plasma have also been demonstrated.[77–83] The exposure of HiPco SWCNTs to a CF_4 plasma produced fluorinated materials with variable stoichiometries,[78] $CF_{0.30-0.63}$ and $CF_{1.25}$, which depended on exposure times ranging from 10 to 60 s (Ref. 78) to 6 min,[77] respectively. While the observed degree of bulk fluorination of SWCNTs was high, the XPS C1s data show the predominant presence of fluorine covalently bonded within the CF_2 and CF_3 groups rather than the C–F ones, which is related to the composition of reactive CF_x species generated in CF_4 plasma. The SWCNTs surface modified by this process have shown a p-type semiconducting behaviour when tested in electronic devices.[78] TEM images showed the partial unroping of SWCNTs achieved by fluorination through CF_4 plasma treatment while FTIR and TGA measurements confirmed the sidewall fluorination of nanotubes. For instance, the C–F covalent bond was represented by the IR absorption band at 1221 cm^{-1} which has been closer to that in fluorographite because of the larger than HiPco-SWCNTs diameter of Arc-SWCNTs ($\sim$2 nm).[52,59]

2. Double-walled carbon nanotubes

Since the fluorination has shown to be a powerful tool for surface modification of SWCNTs, its application was also extended to double-walled carbon nanotubes (DWCNTs). As in the case of SWCNTs, the fluorination studies[84] were motivated by the need for chemical functionalization of DWCNTs which are believed to be more thermally and chemically stable and mechanically stronger than even SWCNTs and due to small diameters (less than 2 nm), they also behave as quantum wires.[85,86] The DWCNTs synthesized by a catalytic CVD method and subsequently purified by HCl treatment and air oxidation[87] were fluorinated by F_2 gas at 200 °C for 5 h. The F/C ratio in the fluorinated DWCNTs was 0.30 according to XPS analysis. The absence of charging effect for fluorinated DWCNTs in comparison with the fluorinated SWCNTs indicated that the inner shells of the DWCNTs most likely remained

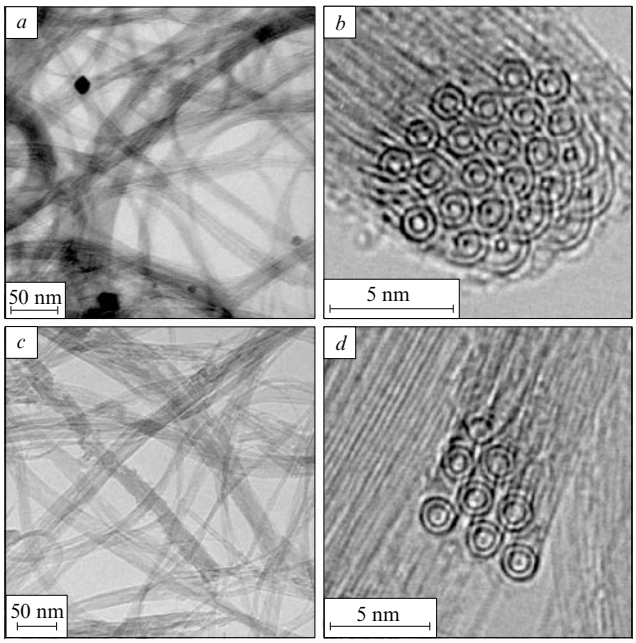


Figure 2. Low-resolution (*a*) and high-resolution cross-sectional (*b*) TEM images of the pristine DWCNTs and low-resolution (*c*) and high-resolution cross-sectional (*d*) TEM images of the fluorinated DWCNTs.[84] (Reproduced on permission of The Royal Society of Chemistry.)

unchanged and maintained conductivity. The C1s and F1s peak positions at 288.9 and 687.75 eV, respectively, confirmed the presence of C—F covalent bonding in fluorinated DWCNTs.

TEM images taken at low-resolution (Fig. 2 *a*) have shown that pristine DWCNTs exist mainly as bundles with the diameters being in the range of 10–50 nm. The high-resolution cross-sectional TEM images of DWCNTs show that they are hexagonally packed within these bundles (see Fig. 2 *b*). Fluorination does not produce a significant change in the macro-morphology of DWCNTs, which remained to be in bundle form (see Fig. 2 *c*). However, it is important to note that fluorinated DWCNTs maintain the integrity of double-layered cylindrical shells, which can be clearly seen, in the high-resolution cross-sectional TEM images (see Fig. 2 *d*). The loosening of hexagonal packing structure was also observed, which indicated that fluorine atoms have been chemically attached to the outer shells of DWCNTs.[84]

Raman spectroscopy was used for structural characterization of fluorinated DWCNTs by observing the changes in the spectral features when compared with the pristine DWCNTs (Fig. 3). The major changes occurred both in the low frequency region (100–350 cm^{-1}) corresponding to radial breathing modes (RBM) and in the high frequency range (1250–1650 cm^{-1}) typical of D and G modes. The RBM frequencies were used for calculation of the tube diameters for the inner and outer shells in DWCNTs, given in Fig. 3 *a*. It is clearly shown that the RBM frequencies below 250 cm^{-1} of outer shells (with the diameters of 1.3 and 1.58 nm) disappear after the fluorination leaving the inner shells with the diameters of 0.70 and 0.90 nm virtually intact. These data provide solid evidence for fluorination of only an outer shell in DWCNTs, each consisting of two concentric tubular shells. The fluorination also causes a slight decrease in the Raman intensity of the G mode band at 1590 cm^{-1} and a dramatic increase of the intensity of the D band at 1346 cm^{-1} (see Fig. 3 *b*) which indicate a structural distortion of the outer shell in DWCNTs due to addition of fluorine and transformation of carbon hybridization from the sp^2 to sp^3 state.

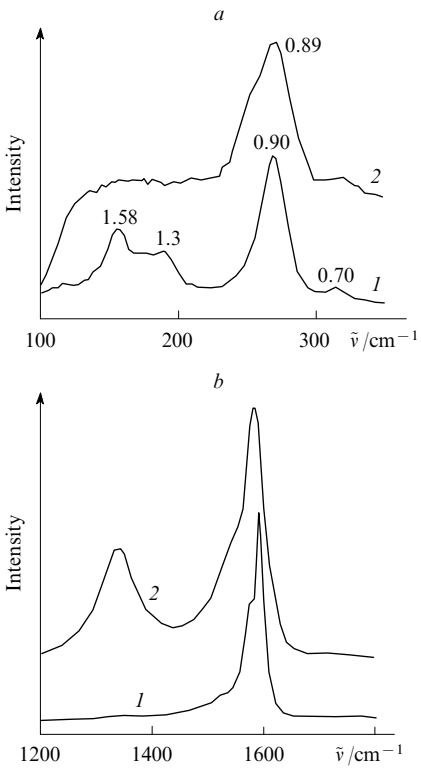


Figure 3. Raman spectra of pristine (*1*) and fluorinated (*2*) DWCNTs (F200) showing a low frequency (*a*) and high frequency (*b*) ranges.[84] (Reproduced on permission of The Royal Society of Chemistry.) The numbers in Fig. 3 *a* correspond to the tube diameter in nm.

In the other studies,[88,89] DWCNTs were also produced from CH_4 by catalytic CVD process, though the diameter distribution was broader than in studies[84,87] ranging from 0.5 to 2.5 nm for the inner tubes and from 1.2 to 3.2 nm for the outer tubes. Fluorination of these nanotubes was carried out by exposing the samples to a vapour over a solution of BrF_3 in Br_2 for 7 days at room temperature. The TEM images of the fluorinated samples have shown that the applied procedure is not destructive to the nanotubes. XPS spectrum exhibited three main peaks due to the C1s, F1s, and O1s features, and very weak peaks showing the presence of small amounts of bromine in the sample. The high-resolution XPS data yielded approximate stoichiometries for several samples, which varied from $CF_{0.20}$ to $CF_{0.35}$, and confirmed a mainly covalent character of bonding of fluorine atoms to the outer shells. Optical and Raman spectroscopy analysis has shown that the inner walls remain intact in fluorinated DWCNTs with the low fluorine content. The increase in concentration of fluorinating agent leads to etching of inner walls in some DWCNTs while nanotubes with the near-armchair configuration were more inert to fluorination.[89]

3. Multi-walled carbon nanotubes

Multi-wall carbon nanotubes (MWCNTs), prepared by a template carbonization method and having the open ends, reacted with elemental fluorine even at 50 °C and were shown to add more fluorine as the reaction temperature increased.[90] When using a gaseous mixture of F_2, HF and IF_5 the fluorination of MWCNTs synthesized by thermal decomposition of acetylene over silica-supported cobalt catalysts proceeded even at room temperature yielding the fluoronanotubes with the $CF_{0.4}$ composition.[91] The C—F bonds in these fluoronanotubes were suggested to possess a semi-ionic character, as indicated by a peak location of the C—F stretch at 1100 cm^{-1} in the FTIR spectra. The X-ray diffraction patterns show the presence of two fluorinated nanotube phases with the interlayer d-spacings of 6.30 and 7.46 Å.

The fluorination of arc-discharge produced MWCNTs has been achieved at room temperature by using elemental fluorine on MWCNT samples pre-treated first with the vapour over liquid Br_2 for 24 h and then with the vapour over a solution of BrF_3 in Br_2 for 7 days.[92] This reaction resulted in fluoronanotubes with the $C_1F_{0.3}Br_{0.02}$ composition, in which the presence of covalent C—F bonds, similar to the C—F bonding in the C_2F fluorographite, has been concluded based on of X-ray diffraction (XRD), FTIR and XPS characterization data. TEM indicated that only the outer shells of MWCNTs were fluorinated while the inner shells remained intact.[93]

Fluorination of MWCNTs prepared by arc-discharge evaporation of spectral graphite rods was also carried out at 420 °C in a nickel reactor by a flow of F_2 diluted with N_2 at the ratio of 1 : 10.[94,95] The fluoronanotubes with the 10 mass %, 15 mass % and 25.4 mass % fluorine content were produced. XRD, IR, XPS, TEM and EELS data suggested that the internal layers are not fluorinated and that some C−F bonds (2%–9%) in fluorinated MWCNTs are ionic. For the fluorinated part of the samples studied, the concentration of fluorine was found to exceed the C_2F composition.[95]

Treatment of MWCNTs with elemental fluorine at room temperature for just 5 min resulted in 4 at.%–5 at.% F addition by formation of predominantly semi-ionic C−F bonds. Low surface coverage by fluorine did not compromise excellent conductivity and magnetic properties of nanotubes and was sufficient to aid excellent dispersion and adhesion of fluorinated MWCNTs in the epoxy matrix which showed increased electromagnetic interference (EMI) shielding due to a well-organized conductive network of nanotubes.[96] This work demonstrates potential for applications of low fluorinated MWCNTs in EMI shielding polymer composites.

Fluorinated MWCNTs with different character of C−F bonding have been obtained at elevated temperature (200 °C) with the use of gas mixtures with variable ratio of elemental fluorine and argon. Analysis of the fluorinated products by XPS has shown that the F (at.%) content increases with the growth of F_2 gas partial pressure in the mixture and the character of C−F bonding changes in the C_xF samples from ionic ($x > 20$) to covalent ($x \leqslant 4$).[97]

Strong dependence of the fluorination on nanotube diameter was observed for MWCNTs produced by thermal decomposition of benzene over Fe catalyst and having diameters ranging from 10 to over 100 nm.[98] After fluorination with the F_2 : HF gaseous mixtures for 19 h at 500 °C these nanotubes revealed the presence of the C−F bonds in the electron energy loss spectra (EELS) only for tubes with diameters larger than 20 nm, which suggested that thin tubes are either not or very little fluorinated. Elemental mapping studies indicated that F is uniformly distributed within the nanotubes with diameters greater than 20 nm of approximately $C_{12}F$ stoichiometry. EELS calculations using density functional theory confirmed the existence of ionic and covalent bonding of fluorine to carbon in these fluoronanotubes.[98]

In a comparative study,[99] MWCNTs of different origin and sidewall morphology, arc-discharge (few surface defects) and catalytic CVD grown (numerous defects), have been fluorinated by a molecular fluorine gas flow at 1 bar and temperature of 520 °C and reaction kinetics has been investigated. Fluorination addition kinetics under these conditions to a saturation level of F/C = 1 was found to correlate with the rate of initial defects in the nanotubes, being faster in case of higher sidewall defects. For instance, after 6 h catalytic tubes become fluorinated up to saturation while arc-discharge tubes remain only partially fluorinated. In comparison to SWCNTs, for which a maximum fluorination temperature of about 300 °C constitutes a critical threshold before degradation starts to occur,[53,60] MWCNTs appear to be much more resistant. It was proposed that this enhanced stability of MWCNTs arises from the reduced curvature of their network and also reflects the key role of relaxation effects in diminishing internal strain within the final fluorinated structure and preventing ruptures along the sidewall. Therefore, it has been suggested that in fluorinated MWCNTs with F/C = 1 saturated stoichiometry, both sides of the curved sheets must be fluorinated to represent rolled homologues of polycarbon fluoride $(CF)_x$ being of interest as perspective nanoscale lubricants.

The use of thermal fluorination with F_2 gas for modification of MWCNTs has enabled potential applications of F-MWCNTs for high performance NO gas sensor electrodes, as demonstrated recently.[100] The NO gas sensitivity was reflected by an increase in electrical resistivity, which was measured to be the highest for the MWCNTs fluorinated at 200 °C. The NO gas sensing mechanism by F-MWCNTs was explained by transfer of electrons from HOMO of NO, adsorbing on F-MWCNTs, to LUMO of F-MWCNTs resulting in increase of Fermi level and eventually causing the resistance increase.[100]

The reaction of MWCNTs, produced by catalytical CVD process, with xenon difluorides has been studied and compared with the results from experiments with elemental fluorine.[101] Fluorination with XeF_2 carried out at room temperature in sunlight or under exposure to the light of a halogen lamp yielded the F-MWCNT material having a 26 : 1 carbon to fluorine ratio. This indicates much lower fluorine content than in the fluoronanotubes produced by elemental fluorine treatment. The XPS studies have confirmed formation of both semi-ionic and covalent C−F bonds, which according to TEM imaging are located only on outer surface of MWCNTs leaving the inner shells intact. It was found that the F-MWCNTs obtained through the reaction with XeF_2 remain electrically conductive with the resistance increased only 5 times in comparison with the reference MWCNT samples.

Treatment of MWCNTs by the CF_4 glow discharge plasma at low pressure resulted in outer walls surface fluorination established by XPS analysis. The fluorinated MWCNTs have shown super-hydrophobic properties according to a water droplet contact angle (CA) measurements, which found the CA value to be about 165°.[102,103]

III. Structure of fluoronanotubes

The structure of fluoronanotubes is governed by the chemical reactivity of particular type carbon nanotube towards fluorine. The reactivity depends on surface curvature, helicity and diameter, and the direction in which the graphene is rolled.[104] Therefore, the fluorination of carbon nanotubes produces different chemical addition patterns, which are influenced by both the difference in fluorine–fluorine interaction, and the strain induced upon the carbon network by forming an sp^3 C−C bonds. The first insight into the fluoronanotube structures has been provided by the molecular modelling calculations and scanning tunnelling microscopy (STM) imaging.[105,106] Based on the experimentally established C_2F stoichiometry at which fluorinated tubes can still maintain their tubular structure, two isomeric structures, resulting from fluorine addition to either (1,2) or (1,4) positions within a hexagonal ring on the graphene-like side wall of the nanotube, have been proposed. Due to the arrangement of the π-bonds, the 1,2-isomer can be conducting through an electron flow along the conjugated bonds parallel to tube axis, whereas the 1,4-isomer with its isolated double bonds will yield insulating fluoronanotubes. From

the molecular mechanics (MM+)[61] and semi-empirical (AM1 and CNDO)[105] calculations it was found that the 1,4-isomer is more stable, although the energy difference between the two isomers is quite small (only 1 kcal mol^{-1} per F atom). Higher level calculations on fluorinated armchair (10,10) SWCNTs of C_2F stoichiometry using density functional theory (PBE/3 and LSDA/3-21G) and periodic boundary conditions[107,108] revealed that, on the contrary, the 1,2-isomer is more stable than the 1,4-isomer; however, the total energy difference is again fairly small (about 4 kcal mol^{-1} per C_2F unit).[108] Given such a small differences in energies of these two isomers calculated at various levels of theory and the absence of separation procedures developed so far, it is reasonable to assume that they both co-exist in the fluoronanotubes material. Based on calculated bandgap values for 1,2 and 1,4-isomers ($\sim$ 1 and 4 eV, respectively), it was concluded that the π-bonding patterns can control the electronic properties of C_2F fluoronanotubes, ranging from metal-like to semiconducting and insulating behaviour, and thus may open possibilities for tailoring these properties through derivatization, providing nanoscale wires, capacitors, and solenoids.[107]

The STM imaging studies indicated that the fluorinated regions typically form bands around the circumference of the tube (Fig. 4). This may imply that the addition of fluorine to the sidewall of the pristine SWCNT should occur more favourably around the circumference of the tube. Nevertheless, the AM1 calculations point out that the addition along the axis of the tube for the 1,2-isomer is about 30 kcal mol^{-1} more exothermic than circumferential 1,2-addition, while in the case of 1,4-isomer the addition around the circumference of the tube is approximately 10 kcal mol^{-1} more energetically favourable than propagation along the tube axis.[61,105] Based on that, the origination of the abrupt band boundaries, observed in the STM images of fluoronanotubes (even those having the saturated C_2F stoichiometry), could be explained by a circumferential addition mechanism proceeding *via* initiation of the 1,4-isomer at multiple sites along the tube and propagating on alternate pairs of rows. However, since the calculated energy difference between the 1,2- and 1,4-isomers is small, the possibility of having both types of fluorine addition to occur simultaneously during the fluorination process also can be expected. Various defects in the sidewall graphene structure might also play an important role in either initiating or terminating such domains.

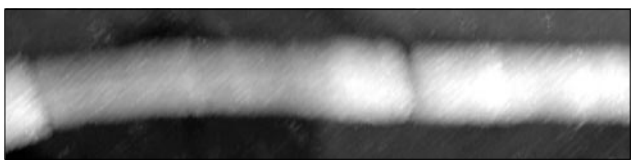


Figure 4. STM image of an individual fluoronanotube.[105]

Higher-level *ab initio* calculations[109] have suggested that fluorine addition in a band-like pattern is stabilized due to electronic confinement effect. These calculations have also shown that for smaller diameter nanotubes axial addition of fluorine is preferred regardless of their chirality. The formation of fluorine bands in fluoronanotubes observed by STM has therefore been explained by axial addition of fluorine in multiple axial C_2F rows rather than randomly in a spot-like pattern. These axial rows are parallel and have matching lengths, which provide a sharp circumferential edge between fluorinated and not fluorinated regions that minimize strain in the fluoronanotubes.[109] The density functional theory studies[110] have shown that the most energetically stable configuration is formed by 1,2-addition of fluorine with the C–F binding energy of 2.43 eV followed by 2.38 and 1.87 eV for 1,4- and 1,3-additions, respectively.

Core and valence band (VB) photoelectron spectroscopy studies of HiPco-SWCNTs fluorinated to approximately C_2F, C_3F and C_4F stoichiometries suggest that these fluoronanotubes are most likely in the armchair configuration.[111] This suggestion is based on better agreement of the experimental and calculated VB spectra for the armchair as compared to zigzag nanotubes. These calculated data provide a set of spectra that can be useful in the interpretation of photoelectron spectra of different fluoronanotube structures. The C1s region of the XPS spectra is the most sensitive to the nanotube structure showing different separation between the two main sp^2 C and sp^3 C(C–F) peaks in the fluoronanotubes of different stoichiometry. This separation increases in the following direction: $C_2F < C_3F < C_4F$ with the smaller separation corresponding to conducting and greater to insulating nanotubes.[112]

IV. Solvation properties of fluoronanotubes

The fluoronanotubes prepared from SWCNTs form metastable solutions in DMF, THF, chloroform, and alcohols after sonication. They do not dissolve in perfluorinated solvents as well as water, diethylamine, and acetic acid. The transmission electron microscopy (TEM) studies show the unroping of fluoronanotubes to a ten times smaller diameter bundles as compared to pristine SWCNTs. The solvation of individual ('unroped') fluoronanotubes was also verified by dispersing them on a mica substrate and examining with atomic force microscopy (AFM).[63,113] The height measurements on the AFM images confirmed that a majority of the observed tubes are individual tubes with the diameter distribution near 0.8 nm.[63] The solutions in alcohols were stable for a few days to over a several weeks. Among the series of alcohols studied, 2-propanol and 2-butanol were found to be the best solvents. Such solvation has been explained by hydrogen bonding between the hydroxyl hydrogen in alcohol and the nanotube-bound fluorine: $R-O-H\cdots F-(C_nF)$. This bonding is likely facilitated by an increased ionic nature of the C–F bond in fluoronanotubes in contrast with alkyl fluorides, in which the fluorine is suggested to be a poor hydrogen bond acceptor.[114] The XPS analysis of fluorinated SWCNTs supports the concept of a more ionic fluorine bonded in fluoronanotubes by revealing an F1s peak at a binding energy of 687–688 eV, located at a much lower binding energy than the F1s peak in poly(tetrafluoroethylene) (691.5 eV).

It should be noted that density functional theory calculations using periodic boundary conditions of the structures of (5,5) and (10,10) armchair C_2F fluoronanotubes indicate that the interaction energies calculated for the $C-F\cdots HOCH_3$ hydrogen bond should be no more than 10% higher than for the $CH_3F\cdots HOCH_3$ linkage. Based on these calculations, it was proposed that the observed sol-

ubility of fluoronanotubes in alcohols is facilitated by combined interaction through both the hydrogen bonds and van der Waals forces.[115]

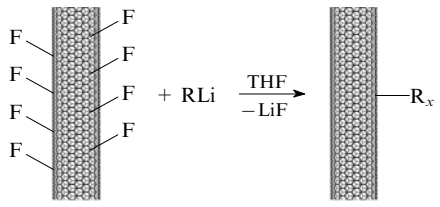
V. Chemical properties of fluoronanotubes

According to DFT calculations of the electronic densities of states, the Fermi energy of the fluoronanotubes is considerably shifted towards lower values compared to the pristine SWCNTs.[116] The conduction bands are energetically lowered as well.[108] This implies that the fluoronanotubes are better electron acceptors than the bare carbon nanotubes and therefore they should more eagerly interact with strong nucleophilic reagents as well as undergo reduction to bare SWCNTs by alkali metals. These chemical reactions are also facilitated by the fact that the C−F bonds in fluoronanotubes as in fluorinated fullerenes are weakened relative to the C−F bonds in alkyl fluorides owing to an eclipsing strain effect,[116,117] and thus fluorine could be more easily displaced. Computational studies have predicted that the mean C−F bond dissociation energies depend very strongly on the nanotube diameter.[116] For example, based on these computations the HiPco SWCNTs should form a stronger bonds with fluorine than the larger diameter L-SWCNTs. Hence, the unique electronic structure and improved solubility of fluoronanotubes and the weaker C−F bond have opened new opportunities for chemical syntheses of a wide variety of sidewall functionalized nanotubes with interesting properties using fluoronanotubes as precursors.

1. Reactions with organolithium and Grignard reagents

The fluorine displacement reactions in F-SWCNTs were first studied with the very strong nucleophiles, such as alkyl lithium and Grignard reagents. These reactions resulted in preparation of a series of short- and long-chain alkyl-SWCNT derivatives.

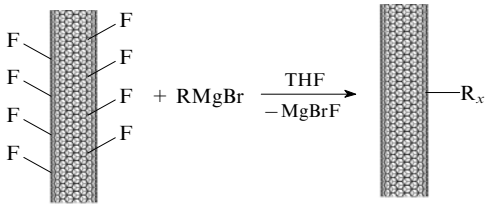
The reactions with organolithium reagents RLi (R = methyl, n-butyl, *tert*-butyl, n-hexyl, phenyl) have been carried out by adding the reagent to the fluoronanotubes dispersed in THF, ether, or hexane, at −40 °C followed by sonication for 10 min and stirring at room temperature overnight under argon. After completion of the workup procedure,[61,118] the final products were dried in a vacuum oven and then characterized by ATR-FTIR, UV-Vis-NIR, TGA and TGA–FTIR techniques.



R = Me, Bu^n, Bu^t, n-C_6H_{13}, Ph.

The ATR-FTIR spectra of the alkylated SWCNTs show the C−H stretching and bending absorptions in the 2850–2970 cm^{-1} and 1000–1470 cm^{-1} regions, typical of alkyl group, respectively, as well as a peak at about 1580 cm^{-1} characterizing the activated C=C stretching mode of the nanotubes. The observed absence of the van Hove electronic transition features in the UV-Vis-NIR spectra supports the occurrence of the sidewall functionalization which dramatically alters the electronic structure of alkylated nanotubes with respect to the pristine SWCNTs. As a result, these alkylated SWCNTs are soluble in common organic solvents such as chloroform and THF. Based on the weight loss at 200–450 °C during the TGA runs, the nanotube carbon-to-alkyl ratios were calculated for methyl, n-butyl and n-hexyl SWCNTs which indicate that alkylation of the fluorinated HiPco-SWCNTs results in a higher degree of functionalization than fluorinated L-SWCNTs. This is in line with the expected enhanced reactivity due to the increased tube curvature. The obtained STM images of the sidewall butylated SWCNTs show that for these derivatives the typical fluoronanotubes banded morphology is no longer visible. Instead, relatively large (~10 Å) bright spots due to sidewall attached butyl groups with an average spacing of ~50 Å are apparent while scanning along the nanotube.[105]

The TGA–FTIR analysis has shown, on the derivative plots, a single maximum for the methylated and two maxima for the n-butylated and n-hexylated SWCNTs, respectively. These maxima were synchronized by the same peaks appearing in the C−H stretching region in the FTIR spectra of volatile products demonstrating the presence of corresponding alkyl groups in the nanotubes and also a likely two-step mechanism of the removal of the alkyl groups, other than methyl. The VTP-MS studies of the methylated SWCNTs have shown that under vacuum conditions the evolution of methyl groups (m/z = 15) is maximized at temperature of about 490 °C, far too high to be due to physisorbed species.[60] The alkylation of the SWCNTs was found to be reversible, since after heating of these materials in Ar at 500 °C a complete recovery of the pristine nanotubes has occurred. Due to the steric effect, *tert*-butyl lithium reacts less effectively and results in a low alkylation and a predominant defluorination of the fluoronanotubes to yield a product showing the van Hove transition bands in the UV-Vis-NIR spectra. Steric effects can also account for more extensive alkylation observed in cases when less sterically demanding alkyl lithium reagents, such as methyl lithium, were used. These results are consistent with a multi-step process that is initiated by a one-electron transfer to the fluoronanotube from the alkyl lithium reagent. Elimination of fluoride from the resulting radical-anion would lead to a radical site on the SWCNT. Recombination of the alkyl radical with this radical site will result in the covalent attachment to the side wall. This step is likely sterically controlled, suggesting that due to crowding of the attaching groups not every fluorine can be replaced by a new functionality, *e.g.*, alkyl group.[118]



R = n-C_6H_{13}, n-$C_{10}H_{21}$, n-$C_{10}H_{20}Br$.

The sidewall alkylation of the fluoronanotubes has also been carried out by reactions with the Grignard reagents (alkylmagnesium bromide) in THF.[119] These reactions were done simply by bath sonication of the fluoronanotube paper

in excess Grignard reagent in THF for several hours. The solubility of the hexylated SWCNTs prepared in such a way in chloroform was up to ~ 0.6 g litre^{-1}, as compared to maximum concentration of 0.1 g litre^{-1} of pristine nanotubes to form stable suspensions in DMF. By heating in air to 250 °C the pristine SWCNTs were recovered from the hexylated derivative for which the attachment of a hexyl group to about 1 in every 10 sidewall carbon atoms has been calculated based on the weight loss monitored by TGA. The analyses of AFM images before and after air oxidation show that the recovered individual tubes are thinner by 2–5 Å after burning off the hexyl groups from side walls. The AFM data also indicate that unlike the partially fluorinated SWCNTs this procedure does not shorten the nanotubes. After removal of the hexyl groups, the two-point electrical resistance measurements across the bucky paper have shown a drop from 372.5 to 144.6 kΩ, a value typical of pristine nanotube papers.

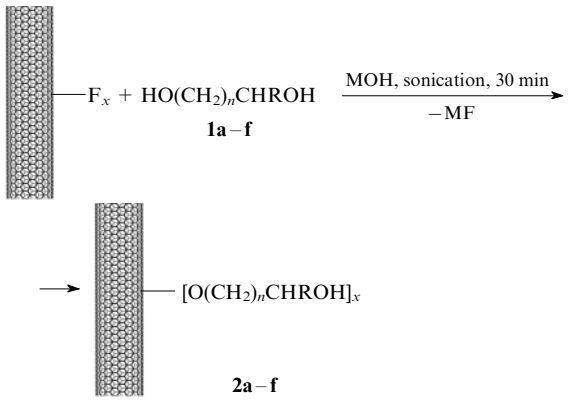
Longer alkyl chain substituents have been attached to the side walls of the SWCNTs by first generating the Grignard reagents from alkyl bromide *in situ*, and then adding the fluoronanotubes.[120, 121] Thus, the n-decylated SWCNTs were prepared by reacting 1-bromodecane with magnesium in ether and then quenching the decylmagnesium bromide with the fluoronanotube suspension in dry ether followed by stirring for 72 h. The TGA in flowing argon has shown an over 40% weight loss due to the evolution of volatile products arising from the n-decyl groups detaching from the SWCNT side walls in the 250–450 °C temperature range. Based on weight loss data, the degree of sidewall functionalization was calculated to be 1 n-decyl group per 15 sidewall carbons.[121]

The reaction of F-SWCNTs with the di-Grignard reagent, prepared in a similar way from 1,10-dibromodecane, also resulted in displacement of fluorine and formation, in this case, of nanotubes cross-linked through $(CH_2)_{10}$ alkane chains. The TGA and TGA–FTIR data indicate loss of attached groups at temperatures of 250–370 °C leading to a recovery of pristine SWCNT features in the Raman and UV-Vis-NIR spectra.[121]

2. Reactions with alkoxide reagents

The solubility of fluoronanotubes (F-SWCNTs) in alcohols prompted their functionalization reactions with the other strong nucleophilic reagents such as alkoxides. For instance, sonication of the fluoronanotubes ($\sim C_2F$) in methanol solution of sodium methoxide for 2 h already resulted in the formation of methoxylated tubes with the $C_{4.4}F(OCH_3)_{0.25}$ composition suggested from electron probe microanalysis (EPMA). Thermal degradation studies by VTP-MS show that under vacuum conditions this product loses significant quantities of methoxy groups ($m/z = 31$) at temperatures of 650–700 °C, indicating that these groups were originally strongly bonded to the nanotube. Based on these data and on elevated oxygen content from the EPMA, the conclusion was made that the methoxy groups are bonded to the nanotube side walls.[113] To follow this work, the derivatization reactions of the fluorinated SWCNTs by methoxy, ethoxy and iso-propoxy groups were also done by sonication in solutions of lithium hydroxide in methanol, ethanol and iso-propanol, respectively.[29]

Based on the established high reactivity of F-SWCNTs towards alkoxides, a simple one-step chemical method for preparation of the SWCNTs functionalized with the hydroxyl group terminated moieties (hydroxyl nanotubes) has been developed. Such method of attaching the functional groups through the sidewall C–O bonding involved reactions of F-SWCNTs with a series of alkane diols and triols pre-treated with the alkali bases MOH.[122] The series included ethylene glycol **1a**, 1,3-propanediol **1b**, 1,4-butanediol **1c**, 1,2-propanediol **1d**, 1,2-butanediol **1e**, and glycerol **1f**. The alcohols, diols and glycerol were used both as solvent media and as reagents to provide a surplus of hydroxyl-terminated monoalkoxides through the reactions with alkali base.

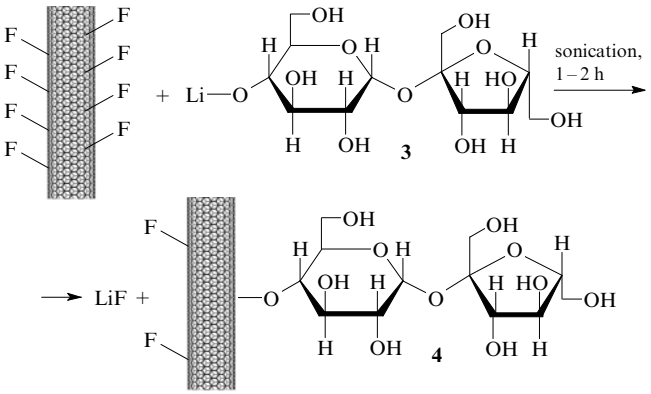


M = Li, Na, K;
R = H: $n = 1$ (**a**), 2 (**b**), 3 (**c**); $n = 1$: R = Me (**d**), Et (**e**), CH_2OH (**f**).

The synthesized 'hydroxyl nanotubes' **2a–f** were characterized by optical spectroscopy, ATR-FTIR, Raman, and UV-Vis-NIR, TEM, AFM, and thermal degradation, TGA and VTP-MS, materials characterization methods. The characterization of 'hydroxyl nanotube' derivatives by Raman spectroscopy has provided essential and quick information for evaluation of the covalent sidewall modification of the nanotubes. The Raman spectra collected for all of these SWCNT derivatives display a peak in the 1285–1300 cm^{-1} region related to the sp^3 states of carbon and serve as a proof of the disruption of the aromatic system of π-electrons on the nanotube sidewalls by the attached functional groups.

The EDX elemental analyses showed 3 at.%–5 at.% residual fluorine content in the derivatives **2a–f**. The degree of sidewall functionalization in **2a–f** was estimated to be in the range of 1 in 15 to 25 carbons, depending on alcohol reagent used. All prepared 'hydroxyl nanotube' SWCNT derivatives have shown an improved solubility in polar solvents as compared to pristine SWCNTs. The solutions of glycerol-SWCNT gerivative **2f** in water (~ 40 mg litre^{-1}) were stable for several days, while ethanol solutions with higher **2f** concentration (~ 80 mg litre^{-1}) showed some precipitation only after several months.[122]

These studies have indicated that the increase in the number of free hydroxyl groups in the moiety attached to the nanotube sidewall should most likely lead to further improvement of the solubilization of functionalized derivatives in polar solvents and water. With this aim in view, the reactions of fluoronanotubes with such readily available polyol reagents as glucose and sucrose have been carried out by using the developed wet chemistry methodology involving sonication technique.[123–125]



Unlike reactions with liquid diols and glycerol, in this method dimethylformamide (DMF) was used as a solvent to separately dissolve solid polyols and F-SWCNTs. To the solution of glucose or sucrose in DMF a lithium hydroxide was added and the mixture was sonicated to form an alkoxide (**3**). The latter was added to DMF solution of F-SWCNTs and sonicated for 1–2 h. The final products, glucose-SWCNT and sucrose-SWCNT (**4**), were isolated by first removing the DMF with rotary evaporator, then dissolving the residue in water and collecting the functionalized SWCNTs on polycarbonate membrane. The FTIR spectra (Fig. 5) of the products of the reactions of fluoronanotubes with glucose- and sucrose-derived alkoxide show strong broad peaks at 3100–3600 cm^{-1} corresponding to the O–H and peaks in the 2800–3000 cm^{-1} range due to C–H stretches of polyol-functionalized SWCNTs. The XPS analysis confirmed that more than a half of fluorine in F-SWCNTs has been either substituted or removed in the course of reaction. Based on TGA weight loss data, the degree of sidewall functionalization by glucose and sucrose moieties (R/C) was estimated to be 1 in 40 to 42 carbons. The SWCNTs derivatized with glucose and sucrose moieties have demonstrated an improved solubility in polar solvents. The SWCNT sucrose derivative **4** was particularly water soluble (~100 mg $litre^{-1}$). The solubility properties are expected to enable applications of sacharide- and other polyol-SWCNT derivatives,[123] which are based on hydrogen bonding ability and chemical reactivity of terminal hydroxyl groups in the side chain.[125]

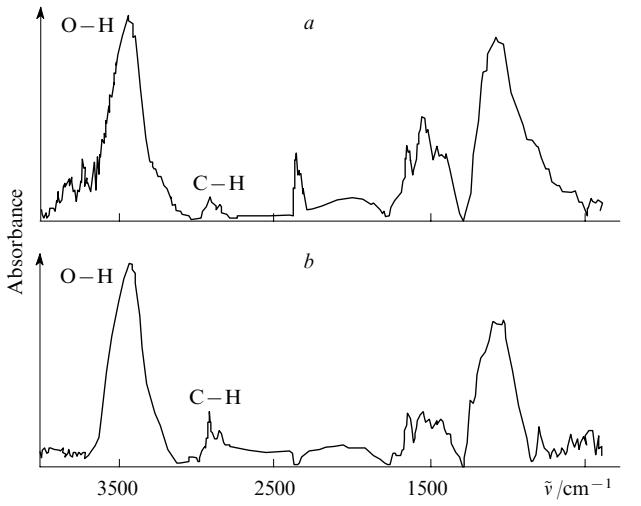


Figure 5. FTIR spectra of glucose-SWCNTs (*a*) and sucrose-SWCNTs (*b*) derived from fluoronanotubes.[125]

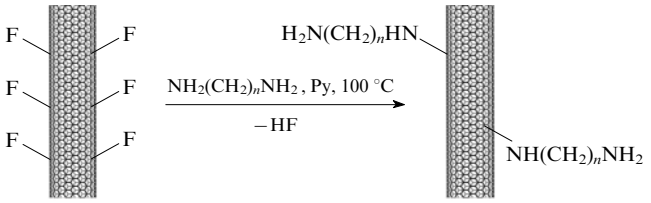
3. Reactions with hydrazine and diamines

The SWCNTs, once fluorinated, can be efficiently defluorinated with anhydrous hydrazine *via* the following reaction:

$$C_nF + \frac{1}{4}N_2H_4 \longrightarrow C_n + HF + \frac{1}{4}N_2,$$

done by stirring at room temperature either in neat or diluted hydrazine or after addition of hydrazine to solutions of fluoronanotubes in organic solvents. The EPMA analysis of the solid precipitate yielded a very low fluorine content, and no nitrogen, confirming that only defluorination and not the functionalization of the SWCNTs by amino moiety has occurred.[29, 60, 119] Such an outcome of this highly exothermic reaction can be explained by the opportunity to produce (in addition to HF) the highly thermodynamically stable N_2 molecules. The AFM studies of pristine, fluorinated and defluorinated SWCNTs have indicated that reagreggation caused by the hydrazine treatment in isopropanol solution does not lead to as large bundles as before the treatment.[63] This defluorination process by hydrazine provides a useful tool for chemical modification of the side walls of the carbon nanotubes, which can be applied for removal of residual fluorine from alkylated fluoronanotubes or for controlled partial defluorination of fluoronanotubes to produce CNTs with various fluorine contents and, presumably, different properties.

Unlike the defluorinating action of hydrazine, the terminal diamines, $H_2N(CH_2)_nNH_2$ ($n = 2, 3, 4, 6$), can be used to functionalize the SWCNTs by creating a direct C–N bonding attachments to the sidewalls. These reactions were performed by refluxing the fluoronanotubes in the corresponding diamine for 3 h in the presence of catalytic amounts of pyridine.[126–129]



The elemental analysis of the washed and dried black precipitates by the EDX yielded a nitrogen content within 11 at.%–16 at.%, and only a very low (1 at.%–2 at.%) fluorine content, suggesting its efficient displacement by the *N*-alkyl amine functionalities. The TGA–FTIR and VTP-MS studies have provided strong evidences for covalent functionalization by the diamines, showing a major loss of the corresponding attached groups at ~350–400 °C, which were detected, for example, in mass spectra by peak at $m/z = 59$ ($HNCH_2CH_2NH_2$) in the case of ethylene diamino-SWCNTs, and by peak at $m/z = 73$ ($HNCH_2CH_2CH_2NH_2$) in the case of propylene diamino-SWCNTs. The TEM images of *N*-alkylaminated samples have also revealed, in addition to the individual sidewall functionalized SWCNTs, a number of the nanotubes cross-linked by the diamino chains, which are more abundant in the case of the larger chain derivatives, hexamethylene

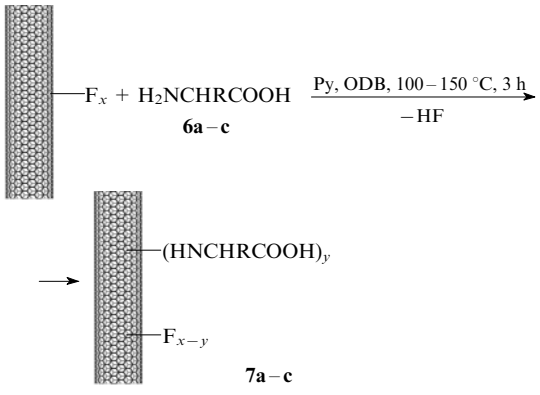
diamino-SWCNTs. It is interesting that Kaiser testing procedure for the free NH_2 groups has tested all *N*-alkyl amine functionalized samples positively. Their availability makes these nanotubes soluble in dilute acids and water and allows them to react, for example, with the adipyl chloride to form new 'nylon tube' materials, as well as to covalently bind to polymer matrixes in nanocomposites or to attach the DNA to the SWCNTs. The developed functionalization route [126–128] using fluoronanotubes and diamines has been effective for fabrication of SWCNT–epoxy composites where the *in situ* produced amino-functionalized SWCNTs were shown to serve under thermal curing conditions both as hardeners and mechanical reinforcers for the epoxy resin [130] and carbon fiber-epoxy matrix interfaces a carbon fiber epoxy composite laminates.[131]

The HiPco SWCNTs fluorinated in a CF_4 plasma under different exposure times were also functionalized with ethylene diamine using the procedure similar to early studies.[127–129] The XPS analysis [78] showed that fluorine substitution reaction was successful and yielded about 7% N content in the functionalized samples thus showing a lower degree of amino functionalization than in the SWCNTs prepared through the methodology described earlier.[126–129]

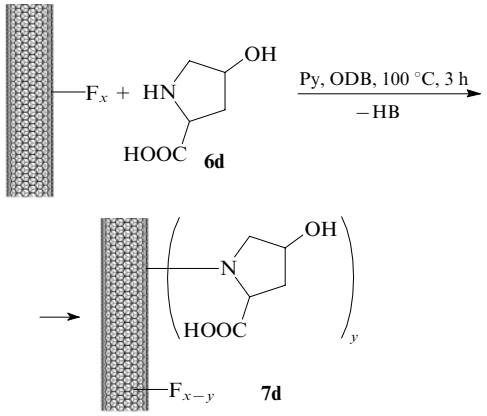
The reaction of F-SWCNTs with diamino (diethyl)-toluene, used commercially as a curing agent (W Cure) for epoxy resins, was also studied.[132] This reaction was found to occur under stirring and heating at 90 °C for 12 h and to result in substitution of most of fluorine groups by aromatic diamine (W Cure) to produce F-SWCNT–$NHC_6H(C_2H_5)_2(CH_3)NH_2$ (**5**) derivative. FTIR, Raman and TGA data provided evidence for covalent attachment to nanotube sidewalls. According to TGA–DTA plot, showing 42% weight loss, the degree of functionalization R/C in **5** was estimated to be ~1 in 20 carbons. This aromatic amino-SWCNT derivative disperses well in DMF solvent and in W Cure itself providing for better compatibility of the nanotubes with the epoxy system and epoxy composite fabrication processing methodology.

4. Reactions with amino acids

Since diamines have shown the ability to react with fluoronanotubes to form sidewall C–N bond, the aminoacids were also chosen to react through their NH_2 end groups with the fluoronanotubes in the presence of pyridine. Several natural α-aminoacids with both protected and unprotected carboxyl groups, such as glycine ethyl ester hydrochloride (**6a**), L-serine ethyl ester hydrochloride (**6b**), L-cysteine (**6c**), and trans-4-hydroxy-L-proline (**6d**), have been studied. By using this route, the nanotube–amino acid derivatives (**7a–d**) were prepared from fluoronanotubes.[133–136]



R = H (**a**), CH_2OH (**b**), CH_2SH (**c**); $x > y$.



ODB is *o*-dichlorobenzene; $x > y$.

This initially reported [133] and patented [134] method has later been reproduced and also extended by other researchers to preparation of nanotubes functionalized with the longer alkyl chain amino acids through reactions of F-SWCNTs with aminocaproic and 11-aminoundecanoic acids.[137]

The amino acid-SWCNT derivatives **7a–d** have been characterized by TGA, Raman, FTIR, XPS, TEM, SEM and AFM techniques. Based on TGA data, the degree of sidewall functionalization in the synthesized SWCNT derivatives was estimated to be in the range of 1 in 8 to 32 carbons, depending on amino acid and reaction temperature used. The ATR-FTIR spectrum of cystein–nanotubes, in particular, shows that the amino acid attached to the SWCNTs adopts a zwitterionic form which is indicated by observation of peaks due to carboxylate and protonated amino groups (Fig. 6). The nanotube–amino acids prepared by this method show improved solubility in water, ethanol, isopropanol, chloroform, and other polar solvents, which is essential for compatibility with bio-systems, polypeptide syntheses, bio-recognition and drug delivery. Their terminal carboxyl groups can also be used for further derivatization and covalent bonding with variety of monomer and polymer matrixes in the processing and fabrication of composites and fibers.

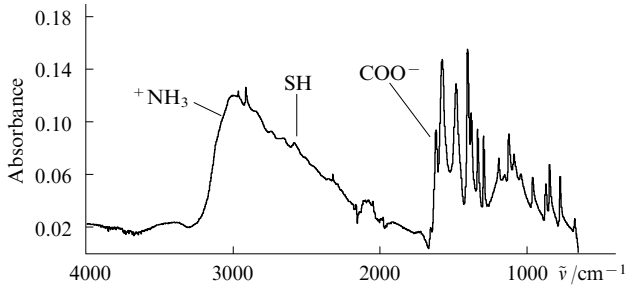
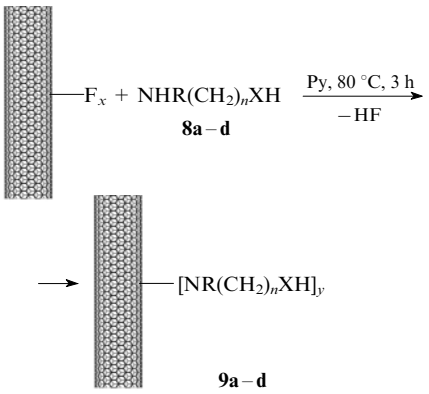


Figure 6. ATR-FTIR spectrum of cysteine–nanotubes.[136]

5. Reactions with amino alcohols and thio derivatives

The method of sidewall C—N modification of fluoronanotubes has also been extended to the other amino group-terminated reagents. For instance, the reactions of fluoronanotubes with amino alcohols, such as 2-aminoethanol **8a**, 3-aminopropanol **8b**, diethanolamine **8c**, and 2-aminoethanethiol **8d** in the presence of pyridine as catalyst yield the hydroxyl group-terminated SWCNT derivatives **9a**–**c**, thus providing another method for synthesis of 'hydroxyl nanotubes'.[122]



X = O, R = H: n = 2 (**a**), 3 (**b**); R = CH_2CH_2OH, n = 2 (**c**);
X = S, R = H, n = 2 (**d**).

In the case of the thiol-SWCNT derivative **9d**, in addition to characterization by Raman, ATR-FTIR and TGA methods, the presence of terminal thiol group on SWCNT sidewalls was established by using the ability of sulfur to form a strong coordination bond with gold. For this purpose the thiol functional groups in **9d** were 'tagged' with 5 nm size gold nanoparticles.

The AFM imaging and height measurements of the single gold 'tagged' nanotube derivative **9d** (Fig. 7) clearly showed the presence of individual gold nanoparticles decorating the side of the nanotube. Direct imaging of the substituents on **9d** was performed by STM analysis after placing the sample onto Au(111) surface. High resolution STM imaging of **9d** showed that multiple functional groups are present on the nanotube in tight bands of approximately 5–25 nm in length.[138] The TGA of **9d** in argon attributed about 35% weight loss to the thiol-terminated groups, which corresponded to a degree of sidewall functionalization R/C of about 1 in 19 carbons.

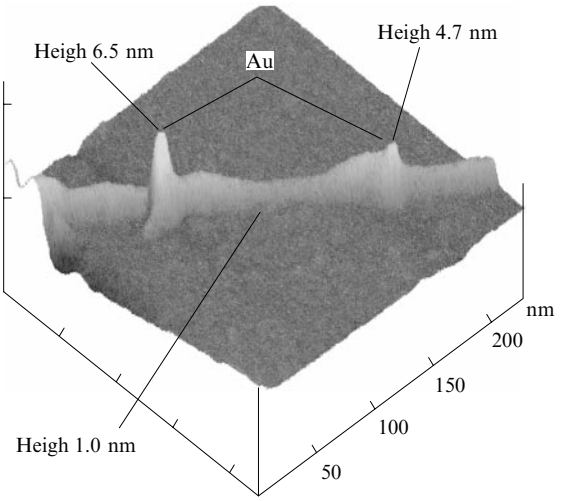
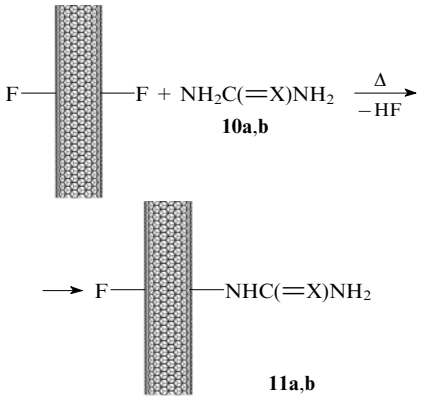


Figure 7. High resolution 3-dimensional AFM image of gold 'tagged' thiol-modified SWCNTs **9d**.[138]

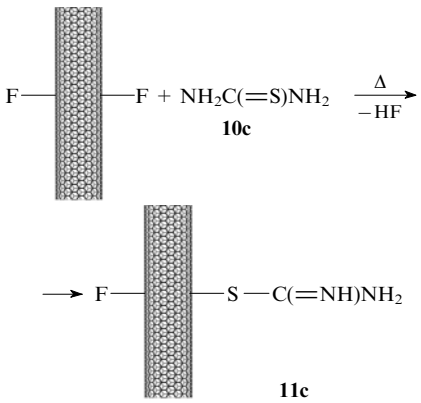
6. Reactions with amides and heteroamides

The functionalization of SWCNTs with the terminal amide and heteroamide functional groups through the reactions of F-SWCNTs with urea (**10a**), guanidine (**10b**) and thiourea (**10c**) is depicted. Low cost, water solubility and chemical properties of these compounds prompt their use as chemical synthons for production of plastics, resins, rubber chemicals, rocket propellants and biomaterials. Besides that, urea, thiourea and guanidine are chaotropic agents, which can cause disruption of local non-covalent bonding in molecular structures, particularly, hydrogen bonding in water. For these reasons, the covalent attachment of simple amide and heteroamide moieties to the SWCNT sidewalls is expected to result in smaller SWCNT bundles and improved dispersion in water and polar organic solvents.

The reactions of F-SWCNTs with amides **10a**–**c** carried out under solvent-free melt (in the case of urea) or DMF solvothermal conditions yielded SWCNT-derivatives **11a**–**c**.[139–142]



X = O (**a**), NH (**b**).



Covalent bonding of amide moieties to the SWCNT sidewall has been confirmed by the use of several materials characterization techniques that showed that the local environment of the fluorine atoms has been modified. Raman spectra of SWCNT-derivatives **11a**–**c** (Fig. 8) have shown shifts in the D peak relative to fluoronanotubes,

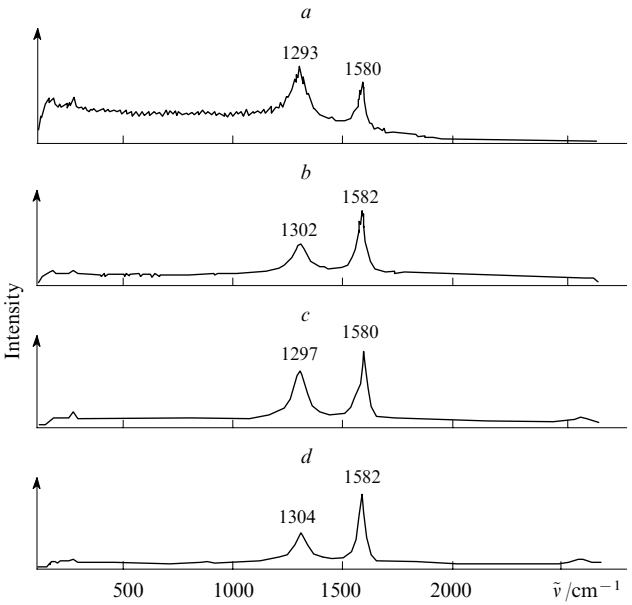
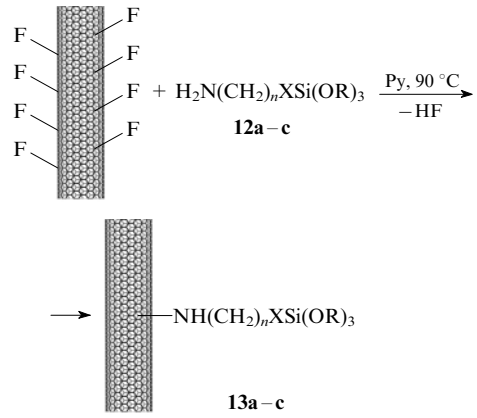


Figure 8. Raman spectra of fluorinated (*a*) and amide-derivatized nanotubes, **11a** (*b*), **11c** (*c*), and **11b** (*d*).[141]

indicating that some other groups have been attached to the sidewall. Also, decrease in the D peak intensity, which indicates an overall reduction of the number of sp^3 C–C bonding sites due to partial defluorination, has been accompanied by the recovery of the sp^2 C=C aromatic bonds between the sites of C–X (X = N, S) bonding of studied molecules to the nanotube sidewalls. FTIR spectra indicated the presence of the characteristic bands of the amide and heteroamide groups as well as decreased intensity of the C–F peaks. TGA–DTA weight loss curves confirmed that fluorine in the F-SWCNTs has been mostly removed and displaced by urea, guanidine and thiourea thus producing a bifunctionalized SWCNT derivatives, bearing residual fluorine and amide functional groups. XPS analysis data have also confirmed the derivatization of F-SWCNTs and shown the amount of residual fluorine (7 at.%–14 at.%), which depended on the functionalization method and reaction conditions used. AFM has shown that urea can form beads of polyurea on the SWCNT sidewall when F-SWCNTs are derivatized through DMF solution method. TEM imaging has directly exposed urea molecules stemming from the sidewalls of derivatized F-SWCNTs. The dispersion of new SWCNT derivatives, U-F-SWCNT, T-F-SWCNT, and G-F-SWCNT, in water and DMF was investigated and stable suspensions were produced.[141, 142]

7. Reactions with aminosilanes

The demonstrated reactivity of the C–F bond in fluorinated nanotubes toward replacement by amino groups, in particular, has facilitated the research work attempting the synthesis of alkoxysilane derivatives of SWCNTs.[82, 143–146] The reactions of F-SWCNTs prepared by fluorination of HiPco-SWCNTs were carried out with the series of aminoalkoxysilanes, such as (3-aminopropyl) triethoxysilane (**12a**), *N*-(2-aminoethyl)-3-aminopropyltrimethoxysilane (**12b**), and *N*-(6-aminohexyl) aminomethyltriethoxysilane (**12c**), in *o*-dichlorobenzene at 90 °C in the presence of small amounts of pyridine.[143, 144]



n = 2: R = Et, X = CH_2 (**a**); R = Me, X = $NH(CH_2)_4$ (**b**);
n = 6, R = Et, X = $HNCH_2$ (**c**).

The obtained SWCNT derivatives (**13a–c**) were characterized by optical spectroscopy, microscopy (AFM and TEM), XPS and TGA methods. Through comparison of the ATR-FTIR spectra of isolated reaction products (Fig. 9) with F-SWCNTs and neat silanes **12a–c**, the removal and displacement of fluorine in F-SWCNTs has been noted and formation of SWCNT silane derivatives **13a–c** was proposed. This has been supported by observation of sharply increased Raman G/D peak ratio and upshift of D-peak in **13a–c** in comparison with F-SWCNTs, indicating substitution of C–F bond by C–N sidewall linkage. XPS analysis showed that after reaction with silanes **12a–c**, the fluorine content has been reduced from 37 at.% in F-SWCNTs to 3 at.%–11 at.% level in **13a–c**. The AFM and TEM produced images show a spiky functional groups attached to the nanotubes.[146]

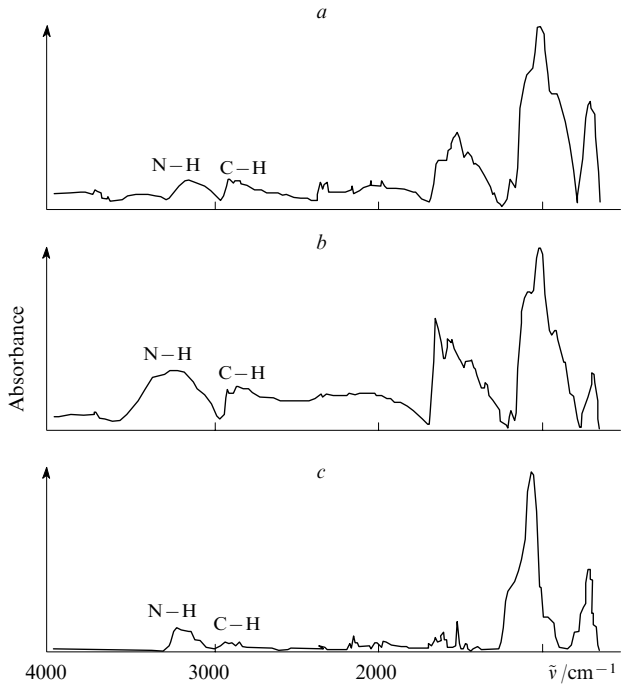


Figure 9. ATR-FTIR spectra of F-SWCNT aminosilane derivatives, **13a** (*a*), **13b** (*b*), and **13c** (*c*).[145]

According to TGA weight loss data, the number of alkoxysilane terminated functional groups attached to the SWCNT sidewalls seems to be decreasing in the direction **13a** > **13b** > **13c** which correlates with the size of aminosilane. The degree of sidewall functionalization by silane groups in **13a** in particular was calculated to be 1 in 11 carbons.

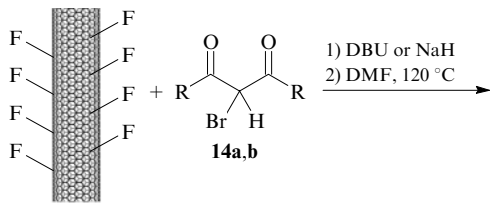
Due to abundance of hydrolyzable alkoxysilane groups SWCNT derivative **13a** has been applied as a precursor for sol–gel synthesis of 0.1 mass % carbon nanotube–silica glass ceramics through dispersion of **13a** in ethanol–tetraethoxysilane mixture followed by gelling in the presence of ammonium hydroxide and then drying in vacuum oven at 100 °C. Uniform dispersion of the functionalized CNT in synthesized silica glass monoliths was confirmed by TEM imaging.[146] In another study,[147] the metal ion chelating ability of SWCNT derivative **13b** through two nitrogen atoms in 1,4-positions of the side chain has been demonstrated by synthesis of **13b**–$CoCl_2$ complex which formed, after hydrothermal treatment, brown-coloured SWCNT–cobalt nanocomposite material. Such incorporation of superstrong lightweight carbon nanotube structures into inorganic matrix, making it biocompatible (bioglass), is of interest in the design of materials with superior mechanical properties for bone tissue engineering.

MWCNTs, fluorinated by analogy with SWCNTs using helium diluted fluorine gas, have also been further derivatized by reaction with the alkoxysilane **12a**.[148] The obtained MWCNT derivative, having 1 in about 30 carbons surface grafting density of silane molecules, was made to react with methyltrimethoxysilane in a sol–gel synthesis, which resulted in poly(methylsilsesquioxane) preceramic material containing well-dispersed MWCNTs covalently bonded to organosilicon polymer matrix. Vacuum pyrolysis of this product was followed by consolidation of obtained ceramic powder by using a spark plasma sintering method which finally produced a MWCNT–silicon oxycarbide ceramic nanocomposite showing 77% increase in elastic modulus with some improvement in fracture toughness.[148]

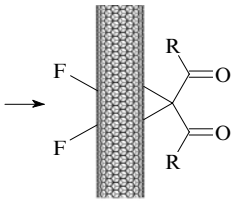
The modification of CF_4 plasma treatment-produced fluoronanotubes with aminosilane **12a** was reported to proceed under sonication at room temperature. It was suggested that covalent bonding of aminosilane to nanotube sidewall could occur under these conditions.[82] However, TEM images did not show any attached molecular chains to the SWCNT sidewalls but only continuous coating on the nanotubes. It appears that this coating consists most likely of siloxane polymer formed during sonication and not the silane covalently bonded to the sidewalls.

8. Bingel reactions

The reactions of fluoronanotubes with bromomalonate reagents **14a**,**b**[149] were carried out by heating in DMF for 3 hours in the presence of strong base, either organic or inorganic, such as 1,8-diazabicyclo(5.4.0)undec-7-ene (DBU) or NaH.



14a,**b**



15a,**b**

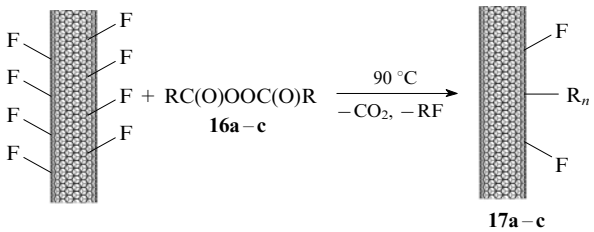
R = $NHCH(CH_2OAc)_2$ (**a**), OEt (**b**).

These reactions resulted in cyclopropanated SWCNT derivatives **15a**,**b**, while pristine SWCNTs remained almost intact under the same reaction conditions and showed the presence of van Hove singularities in the UV-Vis-NIR spectra and very low intensity of the D-mode peak in the Raman spectra. On contrary, the evidence for covalent sidewall attachment in **15a**,**b** was obtained from ATR-FTIR, Raman, variable temperature pyrolysis (VTP)-MS and XPS data. For instance, the FTIR spectrum of **15a** has shown the characteristic peaks of the C=O stretch near 1700 cm^{-1}, the ester C–O and amide C–N stretches at 1300 and 1200 cm^{-1}, respectively. VTP-EIMS studies showed that in comparison with the bromomalonate reagent **14a** itself, which vaporized at 300 °C, the SWCNT derivative **15a** evolved volatile products at temperature as high as 400 °C and above, proving that **14a** is not simply physisorbed by the nanotube. The high resolution XPS C1s spectrum has shown the presence of C–C, C–O, C–N and residual C–F bonds on the nanotubes, also showing that the F content was greatly decreased in comparison with the starting material (fluoronanotube). Bingel reaction was shown to be a useful chemical tool for solubilizing the ultrashort (~20 nm) SWCNTs filled with the MRI contrast agents for medical applications.[150]

9. Reactions with free radical initiators

Since in the fluorinated SWCNTs a large fraction of the sidewall carbons becomes tetrahedral, the bond strain of the residual olefinic moieties is increased as compared with aromatic π-bonds in pristine SWCNTs. In addition, the presence of electron withdrawing substituents further enhances the rate of addition of electron-rich molecules. Thus, the fluoronanotubes may be considered as a source of activated C=C bonds on the SWCNT sidewall. This concept has been verified by studies of the free radical additions and [4+2] Diels–Alder cycloaddition to the fluoronanotubes.

The fluorinated HiPco-SWCNTs have been made to react with lauroyl (**16a**), benzoyl (**16b**), and succinyl (**16c**) peroxides under the same conditions as pristine nanotubes in order to compare the reactivity of their corresponding polyaromatic and conjugated polyene π-systems toward radical addition.[29, 151, 152] All reactions resulted in successful



17a–c

R = n-$C_{11}H_{23}$ (**a**), Ph (**b**), $CH_2CH_2CO_2H$ (**c**).

attachment of undecyl, phenyl and ethyl carboxyl radicals to the sidewalls of fluoronanotubes along with the substantial removal of fluorine to produce SWCNT derivatives **17a–c**.

The addition of undecyl radicals, $C_{11}H_{23}$, generated from lauroyl peroxide **16a**, as well as additions of other radicals proceeded more readily for fluoronanotubes than for pristine SWCNTs, as indicated by a much shorter reaction time (3–8 h *vs.* 5 days) required for observation of prominent C–H stretch peaks in the ATR-FTIR spectra of undecylated fluoronanotubes, in particular. The covalent attachment of long-chain groups to the side walls in the undecyl-derivatized nanotubes was clearly imaged by the TEM (Fig. 10) and confirmed by the TGA–FTIR and VTP-MS data, indicating the major loss of undecyl radicals and their dimer at temperature of about 350–400 °C (peaks in MS at m/z = 155 and 310, respectively).

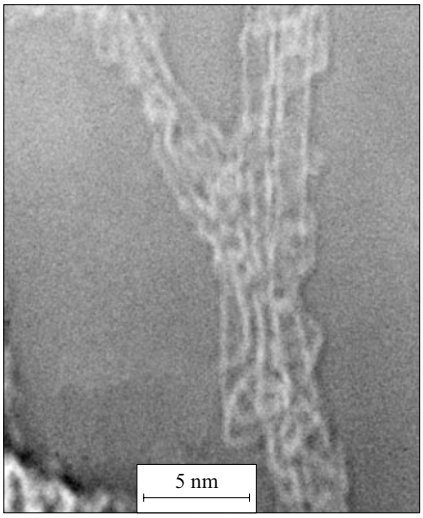


Figure 10. High-resolution TEM image of fluoronanotubes modified by reaction with lauroyl peroxide.[151]

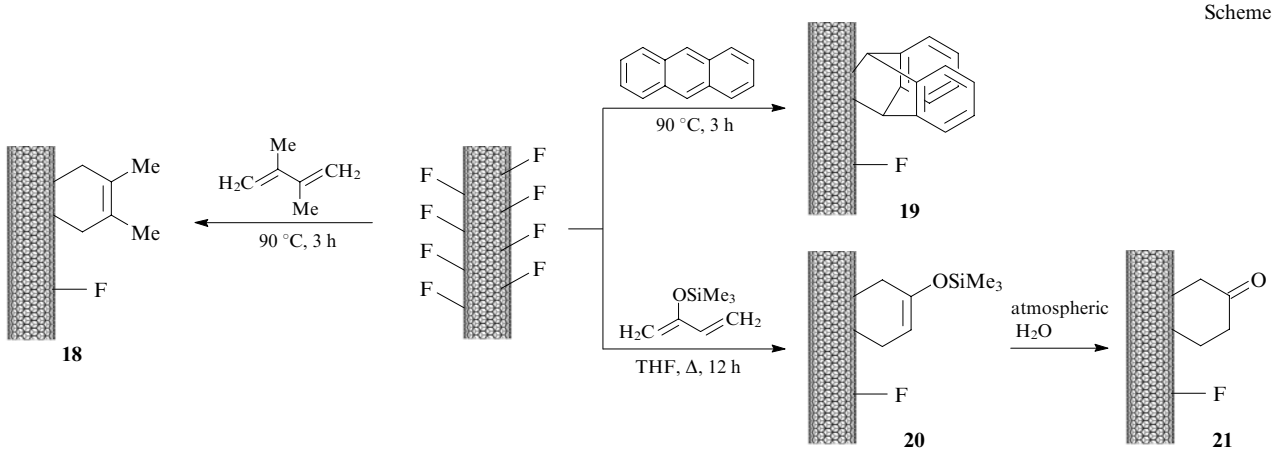
The SWCNT derivative **17a** has been fluorinated for 20 min at room temperature using helium diluted F_2 gas to produce perfluoroalkyl derivative F-SWCNT-$C_{11}F_{23}$-n (**17d**).[153, 154] In the interest of developing a highly sensitive, low power radiation dosimeter, a series of tests were performed on SWCNT-based nanomaterials, which also included bifunctionalized SWCNTs, **17a** and **17c**, to monitor their response to 10 and 30 eV proton radiation.[153] The response to irradiation, measured as a change in resistance, was found to vary with the type of functional group attached to the SWCNT with the larger and more pronounced responses observed for **17a** and **17c**. The nature of the response indicates that these SWCNT nanomaterials may potentially be used for design of dosimeter that is memory-free, reusable, and reversible.

10. Diels–Alder reactions

The fluoronanotubes were shown to undergo a facile reaction with a series of dienes (Scheme 1) that resulted in modified SWCNTs with a high degree of sidewall functionalization.[155] The reactions were carried out with the HiPco SWCNTs which have been fluorinated to an approximately $C_{2.4}F$ stoichiometry. The F-SWCNTs were dispersed in *o*-dichlorobenzene (ODCB) with the assistance of sonication, then either 2,3-dimethyl-1,3-butadiene or anthracene was added and the mixture was heated to 90 °C for 3 hours. Filtration through a 0.2 micron Cole Palmer Teflon membrane, washing with acetone, and drying to 70 °C overnight allowed for the isolation of sidewall functionalized SWCNTs **18** and **19**. The reaction with 2-trimethysiloxyl-1,3-butadiene, to yield SWCNT derivative **20**, was carried out in a similar manner, but in refluxing THF for 12 hours.

The IR, Raman, AFM and ^{13}C NMR characterization were consistent with sidewall functionalization proceeding more efficiently and under milder conditions than in the case of pristine SWCNTs. The C-functional group ratio, as determined from thermogravimetric analysis (TGA), was 21 : 1 (**18**), 32 : 1 (**19**), and 20 : 1 (**20**). The MS characterization of the volatile products from the thermal decomposition of derivatives **18** and **19** was consistent with retro-Diels–Alder reactions. In contrast, and according to the expectations, the TGA/MS of the adduct **20** has shown a fragmentation pattern [m/z = 42 (C_2H_2O); 56 (C_3H_4O); 69 (C_4H_5O); 70 (C_4H_6O)] rather than a retro-cycloaddition. The XPS of the functionalized SWCNTs shows an about 5-fold reduction of the fluorine content in comparison with the precursor (F-SWCNT). The solid state ^{13}C NMR spectrum for SWCNT derivative **18** shows the asymmetric band centred at 111 ppm associated with the unfunctionalized regions of nanotubes as well as a small broad feature at 21 ppm consistent with methyl groups from the Diels–Alder adduct. No peaks associated with the C–F sp^3

Scheme 1



SWCNT carbon have been observed in any of the samples which is consistent with the major loss of the fluorine in the course of reaction.

11. Pyrolysis and cutting of fluoronanotubes

Examination of the products of thermal decomposition of C_2F fluoronanotubes *in vacuo* at temperatures of up to 800 °C by VTP-MS revealed the following species: CF_3^+ ($m/z = 69$), $C_3F_5^+$ ($m/z = 131$), $C_3F_7^+$ ($m/z = 169$) and $C_4F_7^+$ ($m/z = 181$).[60] These data indicate that the pyrolysis of fluoronanotubes is dominated by formation of volatile fluorocarbon molecules and not just the loss of elementary fluorine. Along with the observation of the extended dark bands in the STM images of the partially fluorinated SWCNTs C_nF ($n > 2$) due to bare nanotube sidewalls, these results have led to the idea of using fluorination followed by pyrolysis as chemical 'scissors' for cutting the nanotubes. The process[66,156] implementing this idea involves the fluorination of catalyst-free purified HiPco-SWCNTs to a stoichiometry of C_5F followed by pyrolysis at temperatures up to 1000 °C in an argon atmosphere. This results in cutting the nanotubes at the fluorinated sites to short lengths (20–200 nm). When the pyrolysis process was monitored *in situ* with TGA–FTIR, the fluorine was shown to be driven from the fluoronanotubes structure as CF_4 and COF_2 (due to oxygen covalently attached to the SWCNT sidewall during the first steps of the purification procedure[157]). The same compounds have also been detected by analyzing the volatile products of thermal decomposition of fluoronanotubes by matrix isolation IR spectroscopy and formation of CF_2 and CF_3 species as reactive intermediates has been proposed.[158]

The cut SWCNTs were characterized by Raman spectra, TGA data and AFM images. The latter show their drastically shortened lengths in comparison with the pristine SWCNTs. The average lengths of the cut-SWCNT bundles were about 40 nm. The Raman spectra indicate that cutting of the tubes creates some sidewall defects, which were witnessed by the increased ratio of the integrated D to G mode peaks in comparison with that for purified SWCNTs.[66] High resolution TEM shows that some surface areas of cut SWCNTs (Fig. 11) are partially damaged and appear as a split open pipes. It was also shown that pyrolysis or piranha (H_2SO_4/H_2O_2 mixture) treatment of ozonated F-SWCNTs produces cut nanotubes with the length distribution between 30 and 100 nm, as confirmed by AFM.[159] SWCNTs cut to an array of short lengths are becoming attractive candidates for potential applications including chemically assisted assembly, gas adsorbents, nanocapsules for drug delivery,[150] and polymer composite reinforcements and these studies are in progress.

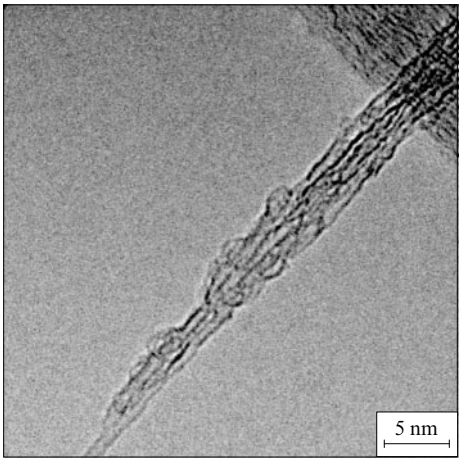


Figure 11. High resolution TEM image of SWCNTs cut through fluorination and subsequent pyrolysis procedure.[69]

Annealing studies[64] have shown that heating of fluoronanotubes $CF_{0.43}$ in He flow caused the largest loss of fluorine, as tested by XPS analysis, at temperatures between 200 and 300 °C and the defluorination was complete at 400 °C. The major change in electrical resistance returning to that of SWCNT material was, however, observed even at 150–200 °C. Raman spectra indicated that upon heating most of the fluoronanotubes revert to SWCNTs which have sidewall defects created by defluorination. AFM imaging showed that defluorinated SWCNT sample consisted of isolated sections shortened in this case to hundreds of nanometers length.

The studies[88] of the thermal behaviour of fluorinated DWCNTs by TGA and XPS has revealed that fluorine removal starts at 100 °C and continues by evolution of fluorocarbon species to completion at 500 °C. The TEM has shown that thermal defluorination does not affect the structure of inner tube shells. However, significant changes in the surface morphology of the outer shell due to alteration of the electronic state of carbon and creation of local defects due to removal of fluorine have been observed. Mass spectrometry studies[89] of fluorinated MCWNTs have shown that under heating in vacuum the evolving gases were composed of CO_2, CO and H_2O in the temperature range from 20 to 120 °C. At higher temperatures, 120 to 300 °C, the evolution of COF_2 was observed, while the CF_4 and C_2F_6 molecules have been detected at 300–450 °C.

Thermal stability of DWCNTs fluorinated by three different methods (gaseous F_2 at 200 °C, mixture of BrF_3 and Br_2 at room temperature, and radio frequency CF_4 plasma) was examined by TGA in an inert atmosphere and by comparing the XPS of pristine samples with those annealed in vacuum at either 70 °C for 10 h or 120 °C for 20 h.[160] The DWCNTs fluorinated by F_2 show the highest stability (the temperature of decomposition is around 396 °C), while the BrF_3 and plasma-fluorinated DWCNTs lose fluorine above 150 °C. Prolonged annealing of the fluorinated DWCNTs in vacuum at a temperature below 150 °C also results in the defluorination of the samples. Fluorine atoms leave the DWCNT surface together with carbon atoms leading to defects in the graphitic network. It is suggested that these defects can become centres for functionalization by oxygen-containing groups during DWCNT storage.

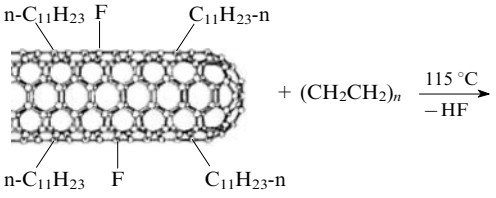
X-Ray absorption near-edge structure spectroscopy has been used for comparative investigation of the electronic structure of pristine and fluorinated SWCNTs before and after annealing.[161] The SWCNTs were produced by catalytic CVD process and fluorinated using a gaseous mixture of BrF_3 and Br_2 at room temperature. The samples were annealed at 250 °C for 0.5 h directly in the vacuum chamber of the X-ray spectrometer. Carbon *K*-edge NEXAFS spectra showed increase in the π-resonance intensity after the treatment of as-produced and fluorinated SWCNTs that was attributed to the detachment of adsorbed molecules and

defunctionalization of nanotubes with the heating. Furthermore, analysis of the spectra revealed the annealing of the SWCNT samples produces topological defects in the nanotube walls.

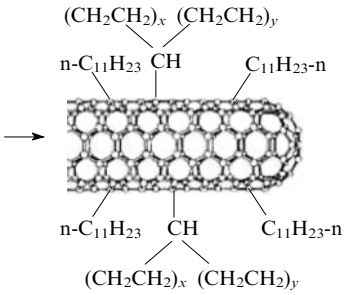
Effect of Ar^+ ion irradiation on the structure of pristine and fluorinated single-wall SWCNTs was examined using TEM, Raman, and XPS.[162] The TEM analysis revealed retention of tubular structures in both irradiated samples while Raman spectroscopy and XPS data pointed at a partial destruction of nanotubes and formation of oxygen-containing groups on the nanotube surface. From similarity of electronic states of carbon in the irradiated pristine and fluorinated SWCNTs observed by XPS, it was suggested that defluorination of nanotubes under Ar^+ ion irradiation proceeded with breaking of C–F bonds.

12. Reactions with the C–H Bonds of polyalkene and polyamide chains

It was found that when fluoronanotubes are mixed with the polyethylene or polypropylene matrix the shortening of nanotubes does not take place under thermal conditions. The TGA–FTIR studies[14] done for F-SWCNT/polyethylene mixture show evolution of HF and lack of any volatile fluorocarbon molecules. The SEM images of TGA residues from fluoronanotubes/polyethylene mixtures show mats of long nanotube ropes. This finding precipitated the idea of possible *in situ* covalent bonding of fluoronanotubes to a polyethylene and polypropylene matrices during polymer melt processing which explained the observed increase in mechanical properties of composites made.[14,15] This idea was further advanced when bifunctional derivative F-SWCNT-$C_{11}H_{23}$ (**17a**), prepared through reaction of fluorinated HiPco-SWCNTs with lauroyl peroxide, was melt-processed with medium density polyethylene (MDPE) in a shear mixer followed by hot pressing.



17a



22

The test samples of polyethylene containing 1 mass % **17a** have shown an almost 3-fold increase in tensile strength. Such considerable improvement of mechanical properties has been explained by entangling of long chain alkyl groups ($C_{11}H_{23}$) with the polyethylene chains during shear mixing. This type of non-covalent interaction provided an additional (to the already proposed *in situ* covalent) interfacial bonding of fluorinated SWCNT derivatives to polyethylene finally producing the integrated SWCNT–polyethylene nanocomposites (**20**).[143,144]

In another study,[154] SWCNT bifunctional derivatives **17a** and **17d** have been prepared from commercial fluoronanotubes (Carbon Nanotechnologies, Inc., currently Unidym) which possessed two times shorter average lengths than F-SWCNTs prepared in the lab from HiPco-SWCNTs. Low aspect ratio of individual nanotubes **17a** and **17d** and their bundles in this case showed a smaller mechanical reinforcing effect on MDPE filled with these nanomaterials[154] than with HiPco-SWCNT analogues.[143,144] Thus, **17a** produced only 15% tensile strength increase while perfluorinated derivative **17d** yielded a higher (52%) enhancement in comparison with the neat MDPE. These results demonstrate the combined effect of nanotube aspect ratio, functionalization and interfacial chemistry on mechanical properties of polyethylene nanocomposites. They show that even decreased aspect ratios can still offer improved mechanical properties if appropriate interfacial chemistry is applied to the nanotube sidewall.[154]

Role of interfacial chemistry involving C–F bonds of fluoronanotube and C–H bonds of organic polymer matrix has also been considered when nylon-6 composite fibre was produced by co-extrusion of polyamide 6 mixed with fluorinated (C_5F) and neat SWCNTs at 220–240 °C.[163] Most dramatic change in mechanical properties of nylon-6 polymer fibers was observed with the addition of 0.5 mass % F-SWCNTs and 1.0 mass % of neat SWCNTs. In each case tensile strength has been increased by 230% as compared to neat nylon-6 fiber. The same order of mechanical reinforcement of nylon 6 achieved by using 2 times lower loads of F-SWCNTs than neat SWCNTs suggests that beside alignment effect of nanotubes in the extruded composite fibre the additional reinforcement is facilitated by interfacial chemical reactions resulting in covalent bonding of fluoronanotubes to polyamide chains.

13. Solid-state reactions with inorganic compounds

Studies of the solid state reactions of fluoronanotubes with the series of binary compounds of Group VA, VIA and VIIA elements[164,165] were prompted by the initial observation of significant reduction of the intensity of the C–F stretch peak in the FTIR spectra of fluorinated SWCNTs pressed into KBr pellets as compared to the ATR-FTIR spectra of neat F-SWCNT samples.[61] When heating a mixture of C_2F fluoronanotubes with KBr at ~120 °C, the evolution of reddish gas was observed, and defluorinated SWCNTs and KF were finally formed as established by the FTIR, Raman and powder XRD analyses of the products and according to a proposed redox reaction:

$$(C_2F)_n + n\,KBr \longrightarrow 2\,C_n + \frac{n}{2}\,Br_2 + KF.$$

The other halides, such as KI, LiI, LiBr, and LiCl have undergone similar transformations, while NaCl and ZnI_2 produced minor changes of the fluoronanotubes.[165] For comparison, fluorinated C_{60} also reacts as an oxidant losing fluorine substantially when heated with KBr, while in the fluorographite CF_x fluorine remains attached to graphite carbons under the same experimental conditions due to the much stronger C–F bonds.[164]

Among the metal compounds of Group VA and VIA elements studied, the sulfide anion in lithium sulfide has

been easily oxidized to elemental sulfur by the fluoronanotubes even at room temperature, while in the case of zinc sulfide prolonged heating (24 h) at 100 °C was required.

The oxides, Li_2O, FeO, PbO and MnO did not react even at 200 °C, while lithium peroxide reacted at room temperature, to form LiF, O_2 and defluorinated SWCNTs. The fluorination of aluminium phosphide by fluoronanotubes to form aluminium trifluoride also took place at room temperature, while the redox reaction with lithium nitride, Li_3N, yielding LiF and N_2, proceeded at 200 °C. In summary, the efficiency of solid state redox reactions of the fluoronanotubes studied is most likely influenced by a combination of two factors (i) the electronegativity of Group VA, VIA and VIIA elements, (ii) the thermodynamic stability of metal fluoride products to be formed. This explains the mild conditions required for these reaction to proceed in the case of lithium halides and a sulfide, and aluminium phosphide, containing the less electronegative elements and producing the very stable fluoride salts, AlF_3 and LiF.

The fluoronanotubes, C_2F, have also been tested for applications as cathodes in a lithium electrochemical cell, for which the discharging performance through a solid state redox reaction has been studied.[166]

$$C_2F + Li \longrightarrow C_2 + LiF.$$

This cell was found to produce a substantially higher voltage than fluorographite CF_x lithium battery commercially used in appliances. Although the discharge of F-SWCNT lithium cell was found to occur during a shorter time than CF_x based one, consistent with the lower fluorine content and a weaker C−F bonds in the fluoronanotubes, the ability to generate a higher power can certainly be useful for a number of applications.

VI. Conclusions

This review demonstrates that during the last 10–15 years fluorination became an important and efficient functionalization tool in carbon nanotube chemistry, materials science and nanotechnology. Fluorine groups attached to the sidewalls of nanotubes prevent the aggregation into bundles due to repulsive interactions. They also enable dispersion and solubilization of nanotubes in organic solvents, providing for the best solubility in alcohols and other polar solvents due to hydrogen bond interaction between hydroxyl protons and fluorine and also van der Waals forces. The solubility of fluoronanotubes, weakened C−F bonds and activated sidewall C=C π-bonds permit a solution-phase chemistry leading to addition reactions and displacement of fluorine by the electron-rich and nucleophilic functional groups. These functional groups also assist in unroping the nanotube bundles and dispersion in polymers and ceramics, crucial for nanocomposites fabrication. The fluoronanotubes thus serve as versatile precursors for novel nanotube derivatives, which in their turn can be used as chemical synthons for new nanoscale materials. As a result, the nanotube derivatives covalently functionalized at the sidewalls show electrical, optical and spectroscopic properties different from pristine nanotubes. The developed methods for chemical cutting of the single-wall carbon nanotubes to 20–200 nanometer lengths involving partial fluorination and pyrolysis of SWCNTs opens additional opportunities for the functionalization chemistry and studies of the length related properties of the cut nanotubes. Various applications of fluorinated and derivatized carbon nanotubes, *e.g.*, in nanocomposites, nanoelectronic devices, nanoengineered drug delivery systems, lubricants and sensors, are already emerging from the continuing chemical research in this interdisciplinary field.

References

1. S Iijima *Nature (London)* **354** 56 (1991)
2. S Iijima, T Ichihashi *Nature (London)* **363** 603 (1993)
3. D S Bethune, C H Kiang, M S de Vries, G Gorman, R Savoy, J Vazquez, R Beyers *Nature (London)* **363** 605 (1993)
4. M Endo, K Takeuchi, S Igarashi, K Kobori, M Shiraishi, H W Kroto *J. Phys. Chem. Solids* **54** 1841 (1993)
5. M S Dresselhaus, G Dresselhaus, P C Eklund *Science of Fullerenes and Carbon Nanotubes* (San Diego, CA: Academic Press, 1996)
6. R Saito, M S Dresselhaus, G Dresselhaus *Physical Properties of Carbon Nanotubes* (London: Imperial College Press, 1998)
7. T W Odom, J-L Huang, P Kim, C M Lieber *J. Phys. Chem. B* **104** 2794 (2000)
8. C N R Rao, B C Satishkumar, A Govindaraj, M Nath *ChemPhysChem*. **2** 78 (2001)
9. R H Baughman, A A Zakhidov, W A de Heer *Science* **297** 787 (2002)
10. M Meyyappan *Carbon Nanotube Science and Applications* (Boca Raton, CA: CRC Press, 2005)
11. J N Coleman, U Khan, Y K Gun'ko *Adv. Mater*. **18** 689 (2006)
12. D McIntosh, V N Khabashesku, E V Barrera *J. Phys. Chem. C* **111** 1592 (2007)
13. J Zhu, H Peng, F Rodriguez-Macias, J L Margrave, V N Khabashesku, A Imam, K Lozano, E V Barrera *Adv. Funct. Mater*. **14** 643 (2004)
14. M L Shofner, V N Khabashesku, E V Barrera *Chem. Mater*. **18** 906 (2006)
15. D McIntosh, V N Khabashesku, E V Barrera *Chem. Mater*. **18** 4561 (2006)
16. J Zhu, A Imam, R Crane, K Lozano, V N Khabashesku, E V Barrera *Compos. Sci. Technol*. **67** 1509 (2007)
17. P-C Ma, N A Siddiqui, G Marom, J-K Kim *Composites, Part A: Appl. Sci. Manufact*. **41** 1345 (2010)
18. R J Chen, S Bangsaruntip, K A Drouvalakis, N W S Kam, M Shim, Y Li, W Kim, P J Utz, H Dai *Proc. Natl. Acad. Sci. USA* **100** 4984 (2003)
19. B Vigolo, A Pénicaud, C Coulon, C Sauder, R Pailler, C Journet, P Bernier, P Poulin *Science* **290** 1331 (2000)
20. M J O'Connell, P Boul, L M Ericson, C B Huffman, Y Huang, E Haroz, C Kuper, J Tour, K D Ausman, R E Smalley *Chem. Phys. Lett*. **342** 265 (2001)
21. A Star, J F Stoddart, D Steuerman, M Diehl, A Boukai, E W Wong, X Yang, S-W Chung, H Choi, J R Heath *Angew. Chem., Int. Ed*. **40** 1721 (2001)
22. A B Dalton, C Stephan, J N Coleman, B McCarthy, P M Ajayan, S Lefrant, P Bernier, W J Blau, H J Byrne *J. Phys. Chem. B* **104** 10012 (2000)
23. R J Chen, Y Zhang, D Wang, H Dai *J. Am. Chem. Soc*. **123** 3838 (2001)
24. A Carrillo, J A Swartz, J M Gamba, R S Kane, N Chakrapani, B Wei, P M Ajayan *Nano Lett*. **3** 1437 (2003)
25. D Nepal, K E Geckeler, in *Interactions of Carbon Nanotubes with Biomolecules: Advances and Challenges in Advanced Nanomaterials* Vol. 2 (Eds K E Geckeler, H Nishide) (Weinheim: Wiley-VCH, 2010) p. 715
26. J L Bahr, J M Tour *J. Mater. Chem*. **12** 1952 (2002)

27. E G Rakov *Rus. Chem. Rev.* **70** 827 (2001); *Usp. Khim.* **70** 934 (2001)
28. A Hirsch *Angew. Chem., Int. Ed.* **41** 1853 (2002)
29. V N Khabashesku, W E Billups, J L Margrave *Acc. Chem. Res.* **35** 1087 (2002)
30. V N Khabashesku, J L Margrave, in *Encyclopedia of Nanoscience and Nanotechnology* Vol. 1 (Ed. H S Nalwa) (Stevenson Ranch, CA: American Scientific Publ., 2004) p. 849
31. A Hirsh, O Vostrowsky *Top. Curr. Chem.* **245** 193 (2005)
32. S Banerjee, T Hemraj-Benny, S S Wong *Adv. Mater.* **17** 17 (2005)
33. V N Khabashesku, J L Margrave, E V Barrera *Diamond Relat. Mater.* **14** 859 (2005)
34. V N Khabashesku, M X Pulikkathara *Mendeleev Commun.* 61 (2006)
35. A Krueger, M Monthioux, in *Strained Hydrocarbons* (Ed. H Dodziuk) (Weinheim: Wiley-VCH, 2009) p. 335
36. V Mittal, in *Advances in Surface Functionalization of Carbon Nanotubes in Polymer Nanocomposites* (Ed. V Mittal) (Hauppauge, NY: Nova Science, 2009) p. 153
37. Y Zhang, Y Bai, B Yan *Drug Discov. Today* **15** 428 (2010)
38. E Vazquez, M Prato *Pure Appl. Chem.* **82** 853 (2010)
39. G Ciofani, V Raffa *Mini-Rev. Med. Chem.* **9** 1251 (2009)
40. L Meng, C Fu, Q Lu *Prog. Nat. Sci.* **19** 801 (2009)
41. S Singh, P Kruse *Int. J. Nanotechnol.* **5** 900 (2008)
42. J Yan, H Zhou, P Yu, L Su, L Mao *Adv. Mater.* **20** 2899 (2008)
43. A M Herrero, M Prato *Mol. Cryst. Liq. Cryst.* **483** 21 (2008)
44. C Lynam, A I Minett, S E Habas, S Gambhir, D L Officer, G G Wallace *Int. J. Nanotechnol.* **5** 331 (2008)
45. A Hirsch, O Vostrowsky, in *Functional Organic Material* (Eds T J Mueller, J J Thomas, U H F Bunz) (Weinheim: Wiley-VCH, 2007) p. 3
46. C M Homenick, G Lawson, A Adronov *Polym. Rev.* **47** 265 (2007)
47. D Cui *J. Nanosci. Nanotechnol.* **7** 1298 (2007)
48. S Campidelli, C Klumpp, A Bianco, D M Guldi, M Prato *J. Phys. Org. Chem.* **19** 531 (2006)
49. F Mercuri, A Sgamellotti *Inorg. Chim. Acta* **360** 785 (2007)
50. K Teker, R Sirdeshmukh, K Sivakumar, S Lu, E Wickstrom, H-N Wang, T Vo-Dinh, B Panchapakesan *NanoBioTechnology* **1** 171 (2005)
51. M Burghard *Small* **1** 1148 (2005)
52. T Nakajima *Fluorine-Carbon and Fluoride-Carbon Materials* (New York: Marcel Dekker, 1995)
53. E T Mickelson, C B Huffman, A G Rinzler, R E Smalley, R H Hauge, J L Margrave *Chem. Phys. Lett.* **296** 188 (1998)
54. A Thess, R Lee, P Nikolaev, H Dai, P Petit, J Robert, C Xu, Y H Lee, S G Kim, A G Rinzler, D T Colbert, G E Scuseria, D Tománek, J E Fischer, R E Smalley *Science* **273** 483 (1996)
55. J Liu, A G Rinzler, H Dai, J H Hafner, R K Bradley, P J Boul, A Lu, T Iverson, K Shelimov, C B Huffman, F Rodriguez-Macias, Y-S Shon, T R Lee, D T Colbert, R E Smalley *Science* **280** 1253 (1998).
56. P Nikolaev, M J Bronikowski, R K Bradley, F Rohmund, D T Colbert, K A Smith, R E Smalley *Chem. Phys. Lett.* **313** 91 (1999)
57. M J Bronikowski, P A Willis, D T Colbert, K A Smith, R E Smalley *J. Vac. Sci. Technol., A* **19** 1800 (2001)
58. Y S Park, K S Kim, K J Jeong, W S Kim, J M Moon, K H An, D J Bae, Y S Lee, G-S Park, Y H Lee *Synth. Met.* **126** 245 (2002)
59. R J Lagow, R B Badachhape, J LWood, J L Margrave *J. Chem. Soc., Dalton Trans.* 1268 (1974)
60. E T Mickelson, Ph.D. Thesis in Chemistry, Rice University, Houston, TX, 1999
61. I W Chiang, Ph D Thesis in Chemistry, Rice University, Houston, TX, 2001
62. N G Lebedev, I V Zaporotskova, L A Chernozatonskii *Int. J. Quantum Chem.* **96** 142 (2004)
63. P R Marcoux, J Schreiber, P Batali, S Lefrant, J Renouard, G Jacob, D Albertini, J-Y Mevellec *Phys. Chem. Chem. Phys.* **4** 2278 (2002)
64. P E Pehrsson, W Zhao, J W Baldwin, C Song, J Liu, S Kooi, B Zheng *J. Phys. Chem. B* **107** 5690 (2003)
65. S Kawasaki, K Komatsu, F Okino, H Touhara, H Kataura *Phys. Chem. Chem. Phys.* **6** 1769 (2004)
66. Z Gu, H Peng, R H Hauge, R E Smalley, J L Margrave *Nano Lett.* **2** 1009 (2002)
67. L G Bulusheva, A V Okotrub, T A Duda, E D Obraztsova, A L Chuvilin, E M Pazhetnov, A I Boronin, U Dettlaff-Weglikowska, in *Nanoengineered Nanofibrous Materials (NATO Sci. Ser. II: Mathematics, Physics and Chemistry)* Vol. 169 (Eds S Guceri, Y G Gogotsi, V Kuznetsov) (New York: Springer, 2004) p. 145
68. Yu V Lavskaya, L G Bulusheva, A V Okotrub, N F Yudanov, D V Vyalikh, A Fonseca *Carbon* **47** 1629 (2009)
69. R L Vander Wal, K Miyoshi, K W Street, A J Tomasek, H Peng, Y Liu, J L Margrave, V N Khabashesku *Wear* **259** 738 (2005)
70. L B Alemany, L Zhang, L Zeng, C L Edwards, A R Barron *Chem. Mater.* **19** 735 (2007)
71. K H An, J G Heo, K G Jeon, D J Bae, C Jo, C W Yang, C-Y Park, Y H Lee, Y S Lee, Y S Chung *Appl. Phys. Lett.* **80** 4235 (2002)
72. Y S Lee, T H Cho, B K Lee, J S Rho, K H An, Y H Lee *J. Fluorine Chem.* **120** 99 (2003)
73. A P Dementjev, A V Eletskii, K I Maslakov, E G Rakov, V F Sukhoverhov, A V Naumkin *Fullerenes, Nanotubes, Carbon Nanostruct.* **14** 287 (2006)
74. A V Krestinin, A P Kharitonov, Yu M Shul'ga, O M Zhigalina, E I Knerel'man, M Dubois, M M Brzhezinskaya, A S Vinogradov, A B Preobrazhenskii, G I Zvereva, M B Kislov, V M Martynenko, I I Korobov, G I Davydova, V G Zhigalina, N A Kiselev *Ros. Nanotekhnol.* **4** 115 (2009) [a]
75. C-M Yang, K H An, J S Park, K A Park, S C Lim, S-H Cho, Y S Lee, W Park, C Y Park, Y H Lee *Phys. Rev. B* **73** 075419 (2006)
76. W I Choi, S Park, T-E Kim, N Park, K-R Lee, Y H Lee, J Ihm, S Han *Nanotechnology* **17** 5862 (2006)
77. B N Khare, P Wilhite, M Meyyappan *Nanotechnology* **15** 1650 (2004)
78. N O V Plank, G A Forrest, R Cheung, A J Alexander *J. Phys. Chem. B* **109** 22096 (2005)
79. N O V Plank, L Jiang, R Cheung *Appl. Phys. Lett.* **83** 2426 (2003)
80. L Valentini, I Armentano, F Mengoni, D Puglia, G Pennelli, J M Kenny *J. Appl. Phys.* **97** 114320 (2005)
81. L Valentini, D Puglia, I Armentano, J M Kenny *Chem. Phys. Lett.* **403** 385 (2005)
82. L Valentini, J Macan, I Armentano, F Mengoni, J M Kenny *Carbon* **44** 2196 (2006)
83. K Shoda, H Kohno, Y Kobayashi, D Takagi, S Takeda *J. Appl. Phys.* **104** 113529 (2008)
84. H Muramatsu, Y A Kim, T Hayashi, M Endo, A Yonemoto, H Arikai, F Okino, H Touhara *Chem. Commun.* 2002 (2005)
85. S Bandow, M Takizawa, K Hirahara, M Yudasaka, I Iijima *Chem. Phys. Lett.* **337** 48 (2001)
86. M Endo, T Hayashi, H Muramatsu, Y A Kim, H Terrones, M Terrones, M S Dresselhaus *Nano Lett.* **4** 1451 (2004)
87. Y A Kim, H Muramatsu, T Hayashi, M Endo, M Terrones, M S Dresselhaus *Chem. Phys. Lett.* **398** 87 (2004)
88. L G Bulusheva, P N Gevko, A V Okotrub, Yu V Lavskaya, N F Yudanov, L I Yudanova, O G Abrosimov, E M Pazhetnov, A I Boronin, E Flahaut *Chem. Mater.* **18** 4967 (2006)

89. P N Gevko, L G Bulusheva, A V Okotrub, N F Yudanov, I V Yushina, K A Grachev, A M Pugachev, N V Surovtsev, E Flahaut *Fullerenes, Nanotubes, Carbon Nanostruct*. **14** 233 (2006)
90. Y Hattori, Y Watanabe, S Kawasaki, F Okino, H Touhara, B K Pradhan, T Kyotani, A Tomita, in *The International Symposium on Carbon Science and Technology for New Carbons (Extended Abstracts of Reports), Tokyo, 1998* p. 180
91. A Hamwi, H Alvergnat, S Bonnamy, F Béguin *Carbon* **35** 723 (1997)
92. A V Okotrub, N F Yudanov, A L Chuvilin, I P Asanov, Yu V Shubin, L G Bulusheva, A V Gusel'nikov, I S Fyodorov *Chem. Phys. Lett*. **322** 231 (2000)
93. N F Yudanov, A V Okotrub, Yu V Shubin, L I Yudanova, L G Bulusheva, A L Chuvilin, J-M Bonard *Chem. Mater*. **14** 1472 (2002)
94. Yu M Shul'ga, V E Muradyan, V M Martynenko, B P Tarasov, N V Polyakova *Fullerenes, Nanotubes, Carbon Nanostruct*. **14** 243 (2006)
95. O M Salamov, F A Abbasova, P F Rzaev *Al't. Energet. Ekol*. (10) 30 (2006) [b]
96. J S Im, I J Park, S J In, T Kim, Y-S Lee *J. Fluorine Chem*. **130** 1111 (2009)
97. J-M Lee, S J Kim, J W Kim, P H Kang, Y C Nho, Y-S Lee *J. Ind. Eng. Chem*. **15** 66 (2009)
98. T Hayashi, M Terrones, C Scheu, Y A Kim, M Rühle, T Nakajima, M Endo *Nano Lett*. **2** 491 (2002)
99. F Chamssedine, D Claves *Chem. Phys. Lett*. **454** 252 (2008)
100. J S Im, S C Kang, B C Bai, T-S Bae, S J In, E Jeong, S-H Lee, Y-S Lee *Carbon* **49** 2235 (2011)
101. E Unger, M Liebau, G S Duesberg, A P Graham, F Kreupl, R Seidel, W Hoenlein *Chem. Phys. Lett*. **399** 280 (2004)
102. Y C Hong, H S Uhm *Appl. Phys. Lett*. **88** 244101 (2006)
103. Y C Hong, D H Shin, H S Uhm *Surf. Coat. Technol*. **201** 5025 (2007)
104. S Park, D Srivastava, K Cho *Nano Lett*. **3** 1273 (2003)
105. K F Kelly, I W Chiang, E T Mickelson, R H Hauge, J L Margrave, X Wang, G E Scuseria, C Radloff, N J Halas *Chem. Phys. Lett*. **313** 445 (1999)
106. N N Breslavskaya, P N D'yachkov *Zh. Neorg. Khim*. **45** 1830 (2000) [c]
107. G Seifert, T Köhler, T Frauenheim *Appl. Phys. Lett*. **77** 1313 (2000)
108. K N Kudin, H F Bettinger, G E Scuseria *Phys. Rev. B* **63** 045413 (2001)
109. G Van Lier, C P Ewels, F Zuliani, A De Vita, J-C Charlier *J. Phys. Chem. B* **109** 6153 (2005)
110. C P Ewels, G Van Lier, J-C Charlier, M I Heggie, P R Briddon *Phys. Rev. Lett*. **96** 216103 (2006)
111. Y-Q Wang, P M A Sherwood *Chem. Mater*. **16** 5427 (2004)
112. N Ranjan, G Seifert *Phys. Rev. B* **73** 153408 (2006)
113. E T Mickelson, I W Chiang, J L Zimmerman, P J Boul, J Lozano, J Liu, R E Smalley, R H Hauge, J L Margrave *J. Phys. Chem. B* **103** 4318 (1999)
114. J D Dunitz, R Taylor *Chem.–Eur. J*. **3** 89 (1997)
115. H F Bettinger *ChemPhysChem*. **6** 1169 (2005)
116. H F Bettinger, K N Kudin, G E Scuseria *J. Am. Chem. Soc*. **123** 12849 (2001)
117. R Taylor *Izv. Akad. Nauk, Ser. Khim*. 852 (1998) [d]
118. R K Saini, I W Chiang, H Peng, R E Smalley, W E Billups, R H Hauge, J L Margrave *J. Am. Chem. Soc*. **125** 3617 (2003)
119. P J Boul, J Liu, E T Mickelson, C B Huffman, L M Ericson, I W Chiang, K A Smith, D T Colbert, R H Hauge, J L Margrave, R E Smalley *Chem. Phys. Lett*. **310** 367 (1999)
120. I Tonks, B McClain, Z Gu, V N Khabashesku, J L Margrave, in *The Rice Quantum Institute Fifteenth Annual Summer Research Colloquium (Abstracts of Reports), Houston, TX, 2001* p. 19
121. I Tonks, D Edman, Z Gu, V N Khabashesku, J L Margrave, in *The Rice Quantum Institute Seventeenth Annual Summer Research Colloquium (Abstracts of Reports), Houston, TX, 2003* p. 18
122. L Zhang, V U Kiny, H Peng, J Zhu, R F M Lobo, J L Margrave, V N Khabashesku *Chem. Mater*. **16** 2055 (2004)
123. Appl. US 20100317820 (2008)
124. O V Kuznetsov, R F M Lobo, V N Khabashesku, in *The Rice Quantum Institute 21st Annual Summer Research Colloquium (Abstracts of Reports), Houston, TX, 2007* p. 2
125. O V Kuznetsov, M X Pulikkathara, R F M Lobo, V N Khabashesku *Izv. Akad. Nauk, Ser. Khim*. 1462 (2010) [d]
126. A Y Huang, I W Chiang, V N Khabashesku, J L Margrave, in *The Rice Quantum Institute Fifteenth Annual Summer Research Colloquium (Abstracts of Reports), Houston, TX, 2001* p. 18
127. J L Stevens, A Y Huang, H Peng, I W Chiang, V N Khabashesku, J L Margrave *Nano Lett*. **3** 331 (2003)
128. J L Stevens, V Kiny, A Y Huang, I W Chiang, G A Derrien, V N Khabashesku, J L Margrave *Proc. NanoTech*. **3** 169 (2003)
129. Int. Pat. 200660171874 (2006)
130. J Zhu, J Kim, H Peng, J L Margrave, V N Khabashesku, E V Barrera *Nano Lett*. **3** 1107 (2003)
131. D C Davis, J W Wilkerson, J Zhu, D O O Ayewah *Compos. Struct*. **92** 2653 (2010)
132. V N Khabashesku, M X Pulikkathara, O V Kuznetsov, in *The 44th Annual Technical Meeting, Society of Engineering Science (Abstracts of Reports), College Station, TX, 2007*
133. H Peng, P Reverdy, V N Khabashesku, J L Margrave, in *The Rice Quantum Institute Seventeenth Annual Summer Research Colloquium (Abstracts of Reports), Houston, TX, 2003* p. 17
134. Int Appl PCT/EP2005/001310
135. V N Khabashesku, in *Extending the Lifespan* (Eds K Sames, S Sethe, A Stolzing) (Münster: LIT Verlag, 2005) p. 245
136. M X Pulikkathara, V N Khabashesku *Izv. Akad. Nauk, Ser. Khim*. 1035 (2008) [d]
137. L Zeng, L Zhang, A R Barron *Nano Lett*. **5** 2001 (2005)
138. L Zhang, J Zhang, N Schmandt, J Cratty, V N Khabashesku, K F Kelly, A R Barron *Chem. Commun*. 5429 (2005)
139. M X Pulikkathara, V N Khabashesku, in *The Rice Quantum Institute 20th Annual Summer Research Colloquium (Abstracts of Reports), Houston, TX, 2006* p. 4
140. M X Pulikkathara, V N Khabashesku, in *The 62nd Southwest Regional Meeting of American Chemical Society (Abstracts of Reports), Houston, TX, 2006* (http://acs.comfex.com/acs/swrm06/techprogram/p37002.HTM)
141. M X Pulikkathara, O V Kuznetsov, V N Khabashesku *Chem. Mater*. **20** 2685 (2008)
142. M X Pilikkathara, Ph.D. Thesis in Applied Physics Rice University, Houston, TX, 2009
143. M X Pulikkathara, V N Khabashesku, in *The Rice Quantum Institute 19th Annual Summer Research Colloquium (Abstracts of Reports), Houston, TX, 2005* p. 8
144. M X Pulikkathara, V N Khabashesku, in *The III Spring Conference. The Associated Nanotechnology Congress Meeting (Abstracts of Reports), Houston, TX, 2005* p. 81
145. Appl. US 20100234503 (2010)
146. A Oki, L Adams, V Khabashesku, Y Edigin, P Biney, Z Luo *Mater. Lett*. **62** 918 (2008)
147. A Oki, L Adams, Z Luo, E Osayamen, P Biney, V Khabashesku *J. Phys. Chem. Solids* **69** 1194 (2008)
148. M D Clark, L S Walker, V G Hadjiev, V N Khabashesku, E L Corral, R Krishnamoorti *J. Am. Ceram. Soc*. (2011) (in the press); DOI: 10.1111/j.1551-2916.2011.04707.x

149. V U Kini, V N Khabashesku, J L Margrave, in *The Rice Quantum Institute Sixteenth Annual Summer Research Colloquium (Abstracts of Reports), Houston, TX, 2002* p. 25
150. J M Ashcroft, K B Hartman, K R Kissell, Yu Mackeyev, S Pheasant, S Young, P A W Van der Heide, A G Mikos, L J Wilson *Adv. Mater.* **19** 573 (2007)
151. H Peng, P Reverdy, V N Khabashesku, J L Margrave *Chem. Commun.* 362 (2003)
152. H Peng, L B Alemany, J L Margrave, V N Khabashesku *J. Am. Chem. Soc.* **125** 15174 (2003)
153. P J Boul, K Turner, J Li, M X Pulikkathara, R C Dwivedi, E D Sosa, Y Lu, O V Kuznetsov, P Moloney, R Wilkins, M J O'Rourke, V N Khabashesku, S Arepalli, L Yowell *J. Phys. Chem. C* **113** 14467 (2009)
154. M X Pulikkathara, O V Kuznetsov, I R G Peralta, X Wei, V N Khabashesku *Nanotechnology* **20** 195602 (2009)
155. L Zhang, J Yang, C L Edwards, L B Alemany, V N Khabashesku, A R Barron *Chem. Commun.* 3265 (2005)
156. Z Gu, H Peng, J L Zimmerman, I W Chiang, V N Khabashesku, R H Hauge, J L Margrave, in *The 223rd ACS National Meeting. Division of Fluorine Chemistry (Abstracts and Papers), Orlando, FL, 2002* p. 12
157. I W Chiang, B E Brinson, A Y Huang, P A Willis, M J Bronikowski, J L Margrave, R E Smalley, R H Hauge *J. Phys. Chem. B* **105** 8297 (2001)
158. H F Bettinger, H Peng *J. Phys. Chem. B* **109** 23218 (2005)
159. Z Chen, Z Gu, K Ziegler, C K Chan, J Shaver, R H Hauge, R E Smalley, in *Proceedings of NSTI Nanotech 2005, Anaheim, CA, 2005* Vol. 2 (Eds M Laudon, B Romanowitcz) (Cambridge, MA: Publ. Nanosci. Technol. Institute, 2005) p. 147
160. L G Bulusheva, Yu V Fedoseeva, A V Okotrub, E Flahaut, I P Asanov, V O Koroteev, A Yaya, C P Ewels, A L Chuvilin, A Felten, G Van Lier, D V Vyalikh *Chem. Mater.* **22** 4197 (2010)
161. Yu V Fedoseeva, L G Bulusheva, A V Okotrub, D V Vyalikh, A Fonseca *Fullerenes, Nanotubes, Carbon Nanostruct.* **18** 595 (2010)
162. Yu V Fedoseeva, L G Bulusheva, A V Okotrub, D V Vyalikh, A Fonseca *J. Chem. Phys.* **133** 224706 (2010)
163. V K Rangari, M Yousuf, S Jeelani, M X Pulikkathara, V N Khabashesku *Nanotechnology* **19** 245703 (2008)
164. R Shukla, B McClain, I W Chiang, V N Khabashesku, J L Margrave, in *The Rice Quantum Institute Fifteenth Annual Summer Research Colloquium (Abstracts of Reports), Houston, TX, 2001* p. 19
165. H Peng, Z Gu, Y Liu, I W Chiang, R E Smalley, R H Hauge, V N Khabashesku, J L Margrave *J. Nanosci. Nanotechnol.* **3** 87 (2003)
166. H Peng, Z Gu, J Yang, J L Zimmerman, P A Willis, M J Bronikowski, R E Smalley, R H Hauge, J L Margrave *Nano Lett.* **1** 625 (2001)

[a] — *Nanotechnol. Russ. (Engl. Transl.)*
[b] — *J. Alt. Energ. Ecol. (Engl. Transl.)*
[c] — *Russ. J. Inorg. Chem. (Engl. Transl.)*
[d] — *Russ. Chem. Bull., Int. Ed. (Engl. Transl.)*